Mechanisms of Solvation Dynamics of Polyatomic Solutes in Polar and Nondipolar Solvents: A Simulation Study

ARTICLE *in* THE JOURNAL OF CHEMICAL PHYSICS · AUGUST 1998

Impact Factor: 2.95 · DOI: 10.1063/1.476911

2 AUTHORS:

Branka M. Ladanyi
Colorado State University
152 PUBLICATIONS **5,138** CITATIONS
SEE PROFILE

Mark Maroncelli
Pennsylvania State University
126 PUBLICATIONS **11,738** CITATIONS
SEE PROFILE

Mechanisms of solvation dynamics of polyatomic solutes in polar and nondipolar solvents: A simulation study

Branka M. Ladanyi
Department of Chemistry, Colorado State University, Fort Collins, Colorado 80523

Mark Maroncelli
Department of Chemistry, The Pennsylvania State University, University Park, Pennsylvania 16802

(Received 15 January 1998; accepted 20 February 1998)

Molecular dynamics (MD) simulations of a benzenelike solute in acetonitrile and CO_2 (298 K and 52.18 cm^3/mol) are used to investigate the molecular basis of solvation dynamics in polar and nondipolar solvents. The solvation response to various charge rearrangements within the benzene solute are simulated in order to mimic the type of electrostatic solvation observed in typical experimental systems. From equilibrium MD simulations the solvation time correlation function [TCF; $C(t)$] and the corresponding solvation velocity TCF [$G(t)$] are used to study the mechanisms underlying time-dependent solvation within the linear response limit. Decomposition of $G(t)$ into contributions from rotational and translational solvent velocities reveals that the relative mix of these two types of motion is quite similar in the two solvents but is strongly dependent on the multipolar order (m) of the solute perturbation. The contribution of translational solvent motions to both the short and long time dynamics of $C(t)$ increases from about 10% for a monopolar perturbation ($m=0$; i.e., a change in net charge) to about 40% for a perturbation of octopolar ($m=3$) symmetry. Decomposition of both $C(t)$ and $G(t)$ into single-molecule and molecular-pair contributions shows that the collective nature of the solvation response depends markedly on the charge symmetry of both the solvent molecule's charge distribution and the solute perturbation. In the nondipolar solvent CO_2 neither $C(t)$ nor $G(t)$ differ significantly from their single-molecule counterparts—collective effects are therefore of little consequence to solvation in this solvent. However, in the highly dipolar solvent acetonitrile pair contributions to $C(t)$ greatly suppress the magnitude of the solvation response and as a consequence greatly increase the speed of the response over what it would be in their absence. The importance of these intermolecular correlations in acetonitrile decreases substantially with m, such that the ''suppression factors'' (α_s) vary from ~ 9 for $m=0$ to ~ 2 for $m=3$. The intermolecular correlations of primary importance in acetonitrile are of a static rather than a dynamic nature (i.e., pair effects on $G(t)$ are of only secondary importance). This feature makes it possible to employ several approximate relationships to relate the collective dynamics of solvation in polar fluids to simpler single-solvent molecule dynamics. © *1998 American Institute of Physics.* [S0021-9606(98)03420-5]

I. INTRODUCTION

Solvation dynamics refers to the rate of solvent reorganization in response to an abrupt change in solute properties. In most experimental studies of this phenomenon, the solute is a chromophore whose charge distribution can be altered via electronic excitation. The temporal response of the solvent to such a perturbation can be monitored through observation of the dynamic Stokes shift of the chromophore's emission spectrum or through various photon echo spectroscopies.[1–7] In many chemical reactions, especially those involving charge transfer, the dynamic solvent response to a solute-induced electrostatic perturbation plays an important role, making solvation dynamics not only interesting in its own right, but an essential prerequisite to understanding the effects of solvents on chemical reactions.[8–12] This connection to chemical reactions, as well as experimental advances which have made it possible to observe solvation dynamics on the subpicosecond timescale, have generated a great deal of interest in this phenomenon. Several reviews[2–7] summarize the recent advances in this field.

Progress in our understanding of the solvation process has come through an interplay of ultrafast laser spectroscopy, theory, and computer simulation. Molecular dynamics (MD) simulations have proven to be especially well suited for modeling the short time dynamics of solvation. For example, it was through simulation that the dominant inertial component of the solvation response in many common liquids such as water,[13–20] acetonitrile,[21–26] and methyl chloride[27] was discovered. Only fairly recently has the importance of this ultrafast component been confirmed through experimental studies.[28–33] Computer simulations are also well suited to the determination of the molecular mechanisms of solvation dynamics. Answers to many mechanistic questions are accessible through the appropriate analysis of MD trajectory data and most of our knowledge about the molecular mechanisms of solvation dynamics stems from such analyses.[34] One of our goals in the present study is to answer several questions

concerning the molecular mechanisms of solvation dynamics: Does the solvent relax mainly through rotation or through translation? Is the solvation process predominantly collective, involving correlated motion of solvent molecules, or does it involve primarily single-solvent dynamics? How does solvation dynamics depend on the range and symmetry of the perturbation in solute-solvent interactions? Is solvation dynamics fundamentally different in dipolar and nondipolar solvents? In this article we investigate these mechanistic questions through the study of polyatomic solutes in acetonitrile and carbon dioxide solvents. Based on the results of our mechanistic studies we propose approximations to the solvation response in terms of simpler, single-molecule solvent dynamics.

With a few notable exceptions,[15,16,18,23,29,30,35–38] most of the theoretical and simulation studies of solvation dynamics have focused on simple model solutes such as monatomic ions and dipolar diatomic molecules which do not closely resemble the large polyatomic chromophores used in experiment. MD simulations indicate that there are significant differences between the solvent's response $[S(t)]$ to polyatomic solutes and simple monatomic or diatomic species.[23,29] For example, Kumar and Maroncelli[23] recently studied the solvation of coumarin 153 (C153), a typical chromophore used in dynamic Stokes shift experiments. Semiempirical electronic structure calculations indicated that the $S_0 \rightarrow S_1$ electronic transition in C153 leads to a rather complicated perturbation of its charge distribution, involving changes in charge on many atoms. Simulations in acetonitrile and methanol,[23] and in water,[30] showed that the solvation response to this type of complex charge redistribution is appreciably slower than it is in the case of a charge or dipole change in atomic ions or diatomic solutes.

In the present work we seek a better understanding of a solvent's response to such complicated solute perturbations, through analysis of the solvation mechanisms for benzene-like solutes undergoing several hypothetical charge perturbations. These same solutes were previously examined in the solvents acetonitrile and methanol by Kumar and Maroncelli,[23] who found that $S(t)$ was mainly dependent on the multipolar order of the solute charge perturbation involved. We have performed additional simulations in acetonitrile as well as new simulations in the nondipolar solvent CO_2 in order to develop further insight into the molecular origins of solute dependence of solvation dynamics.[23,29,30,39,40] We investigate the role of solvent polarity on the solvent response through comparison of the two solvents acetonitrile and CO_2. These two solvents are quite similar in size, shape, and inertial characteristics, but they differ in the symmetry of their charge distributions. CO_2 is representative of a class of solvents possessing no net dipole but which nevertheless contain significantly polar bonds. Such solvents have received comparatively little attention from simulation or theory to date.[41] However, recent experiments[31,42] have shown that solvation of C153 in nondipolar solvents such as benzene and dioxane is comparable in both the size of the fluorescence Stokes shift and in its time evolution to what has been observed in polar solvents. (These studies also showed CO_2 to exhibit a sizable Stokes shift but its dynamics have yet to be measured experimentally.) Analysis of these experiments[42] suggests that solvation in these cases involves primarily solute-solvent electrostatic interactions and therefore should proceed via a mechanism similar to that of polar solvation.[25,26] CO_2 is an obvious choice for computer simulations of solvation dynamics in nondipolar solvents due both to its simplicity and by virtue of the widespread use of supercritical CO_2 as a reaction medium.

For the chromophores used in solvation dynamics experiments, the change in molecular geometry on electronic excitation is small, so that the Stokes shift arises primarily from changes in the solute-solvent interaction potential brought about by solute electronic transition. The dynamical variable monitored in experiment is therefore the energy gap

$$\Delta E = U_{Ss}^1 - U_{Ss}^0, \tag{1.1}$$

where U_{Ss}^1 and U_{Ss}^0 are solute-solvent interaction energies when the solute is in the S_1 and S_0 electronic states. The largest steady-state Stokes shifts are observed for solute-solvent pairs for which ΔE corresponds to a large change in electrostatic interactions, so ΔE is expected to be primarily electrostatic in nature for solvation in systems of most experimental interest. In this work we will focus on electrostatic solvation, but consider solvents with and without permanent dipoles.

In terms of ΔE, the Stokes shift response function is given by

$$S(t) = \frac{\overline{\Delta E(t)} - \overline{\Delta E(\infty)}}{\overline{\Delta E(0)} - \overline{\Delta E(\infty)}}, \tag{1.2}$$

where overbars denote averages over nonequilibrium trajectories in which the system is perturbed by solute electronic excitation occurring at $t=0$. When the perturbation in solute-solvent interactions resulting from solute electronic excitation is small, $S(t)$ can be approximated by its linear-response counterpart, the solvation time correlation function (TCF)

$$C(t) = \frac{\langle \delta\Delta E(0)\, \delta\Delta E(t) \rangle}{\langle (\delta\Delta E)^2 \rangle}, \tag{1.3}$$

where $\delta\Delta E = \Delta E - \langle \Delta E \rangle$ is a fluctuation in ΔE and where $\langle \cdots \rangle$ denotes an ensemble average measured in an equilibrated solute-solvent system. (The solute can be in either of its electronic states for purposes of this equilibrium average.) MD simulations indicate that the approximation $S(t) \cong C(t)$ holds even for fairly large solute perturbations in many solvents,[13–16,21,23] including acetonitrile,[21,23] one of the liquids considered here.

Our approach focuses on analysis of $C(t)$ and of the solvation velocity TCF,

$$G(t) = \langle \Delta\dot{E}(0)\, \Delta\dot{E}(t) \rangle, \tag{1.4}$$

which is related to $C(t)$ by

$$C(t) = 1 - \langle (\delta\Delta E)^2 \rangle^{-1} \int_0^t (t-\tau) G(\tau)\, d\tau. \tag{1.5}$$

The above equation shows that $C(t)$ is governed by static correlations contained in $\langle (\delta\Delta E)^2 \rangle$ as well as by dynamical

correlations contained in $G(t)$. As we shall see, both types of correlations play important roles in the behavior of $C(t)$, with the *static* correlations being chiefly responsible for the short time aspects of its collective character.

Analysis of $G(t)$ is the focus of the instantaneous normal mode (INM) theory of solvation dynamics.[22,24,25,43–48] In that approach one constructs the INM solvation spectrum $\rho_{\mathrm{solv}}(\omega)$, which is approximately related to $G(t)$ by Fourier transformation

$$G(t) \cong k_B T \int d\omega \rho_{\mathrm{solv}}(\omega) \cos\, \omega t. \tag{1.6}$$

The above relation is exact at short times, making INM analysis an especially valuable tool for the investigation of short time solvation dynamics. Using the connection between INM eigenvectors and molecular coordinates and applying projection operator techniques, $\rho_{\mathrm{solv}}(\omega)$ can be decomposed into subspectra resulting from a variety of molecular processes.[22,24,25,43–48] It is through this decomposition that contributions of rotational and translational dynamics to the early solvation response were first determined.[22,24,25] Several other aspects of the solvation mechanism, such as contributions to $\rho_{\mathrm{solv}}(\omega)$ from nearby solvent molecules,[22,46,48] have been determined as well.

Here we adopt a related, but somewhat different approach, not restricted to short time dynamics. It is based on the formalism developed by W. A. Steele[49] for analyzing and approximating collective TCFs. This approach allows us to identify contributions to $G(t)$ from different degrees of freedom, such as molecular translations and rotations, and molecular velocity auto- and cross-correlations. Several previous uses of the Steele theory to obtain mechanistic information about condensed-phase dynamical processes have been reported. They include applications to solvation dynamics,[24,26,48] optical Kerr effect,[24] far-infrared absorption,[50] and vibrational relaxation.[46] Our approach resembles most closely the mechanistic studies reported in Ref. 26. Following the methods that Steele proposed, we also construct and test approximations to $C(t)$ in terms of static intermolecular correlations and simpler solvent dynamics.

A major goal of theoretical studies of solvation dynamics has been to determine how it is related to pure solvent dynamics. Insights into this question can be gained by investigating how and why the solvent's response differs for different solutes, solvents and forms of ΔE. When ΔE is a perturbation in the solute-solvent electrostatic interactions, several pieces of evidence indicate that rotational motion will dominate over translation. Ladanyi and Stratt[22,25] have shown using INM analysis that $C(t)$ at short times decays primarily through rotation when ΔE is a dipole–dipole[22,25] or a quadrupole–quadrupole[25] interaction, but that translation contributes more in the latter than the former case. They have also shown[25] that the contribution of rotation versus translation to the short time solvation response will, in general, depend the symmetry and range of ΔE as well as on the magnitudes of solvent masses and moments of inertia.

The form of ΔE involving interactions of the longest range corresponds to a change in charge of an ionic solute in a polar solvent. The solvent response should then be mainly rotational in character. Indeed Maroncelli, Kumar, and Papazyan[51] have shown that in this case an excellent approximation to $C(t)$ is given by

$$C(t) = [C_1(t)]^{\alpha_1}, \tag{1.7}$$

where

$$C_1(t) = \langle \hat{\mathbf{u}}(0) \cdot \hat{\mathbf{u}}(t) \rangle \tag{1.8}$$

is the orientational TCF of the dipole moment (direction $\hat{\mathbf{u}}$) of a solvent molecule in the absence of the solute. They related the exponent α_1 to solvent polarity and estimated it quite accurately from the solvent dipole density and dielectric constant. Equation (1.7) was not originally intended to apply to nondipolar solvents, but it can be extended to them by interpreting $\hat{\mathbf{u}}$ as a unit vector along, for example, one of the principal axes of the quadrupole tensor of a solvent molecule.[52]

For the solvation response to a change in higher moments of the solute charge distribution, Eq. (1.7) is not expected to apply, but there can still be an approximate connection between single-solvent dynamics and the more collective response measured by $C(t)$. Raineri, Friedman, and co-workers[37,53] have shown that a power-law scaling connection between two TCFs such as $C(t)$ and $C_1(t)$ can be established on the basis of a convolutionless generalized Langevin equation. They have exploited this connection to estimate $C(t)$ from the solvent dielectric permittivity[53] and to relate the solvation responses associated with different forms of ΔE.[37] Castner and Maroncelli[52] have also shown that power-law scaling applies in a very approximate way between the experimentally observed solvation and the optical Kerr effect responses.

Here we develop connections between $C(t)$ and single-solvent and pure-solvent dynamics through Steele theory and test them using our MD simulation results. As a part of this investigation we determine from MD the single-solvent contributions to $C(t)$ and $G(t)$ as well as pure-solvent angular and center-of-mass velocity TCFs.

The remainder of the article is organized as follows: In Sec. II, we describe the model systems studied and provide the details of the MD simulations methods used. Our methods of analysis of the simulation data and definitions of the quantities of interest are given in Sec. III. Our results are presented in Sec. IV and our main findings summarized in Sec. V.

II. MODELS AND METHODS

Data on solvation dynamics are obtained from molecular dynamics (MD) computer simulations. We use site–site intermolecular potentials that are sums of Lennard-Jones (LJ) and Coulomb terms

$$u_{\alpha\beta}(r) = 4(\epsilon_\alpha \epsilon_\beta)^{1/2} \left[\left(\frac{\sigma_\alpha + \sigma_\beta}{2r} \right)^{12} - \left(\frac{\sigma_\alpha + \sigma_\beta}{2r} \right)^{6} \right] + \frac{q_\alpha q_\beta}{4\epsilon_0 \pi r}. \tag{2.1}$$

As indicated in the above equation, the LJ potential parameters for pairs $\alpha\beta$ of unlike sites are obtained from individual

TABLE I. Potential parameters and molecular geometries.

	Solvent: CH_3CN[a]		
Site	$\epsilon_\alpha/(K/k_B)$	σ_α/Å	q_a/e
CH_3	191	3.6	0.269
C	50	3.4	0.129
N	50	3.3	−0.398
	Solvent: CO_2[b]		
Site	$\epsilon_\alpha/(K/k_B)$	σ_α/Å	q_a/e
C	28.129	2.757	0.6512
O	80.507	3.033	−0.3256
	d_{CO}=1.149 Å, d_{OO}=2.298 Å		
	Solute: Benzene[c]		
Site	$\epsilon_\alpha/(K/k_B)$	σ_α/Å	q_a/e
C	40.3	3.50	−0.135
H	25.18	2.50	0.135
	d_{CC}=1.41 Å, d_{HH}=1.09 Å.		

[a]Reference 55.
[b]Reference 56.
[c]Reference 23.

site parameters using Lorentz-Berthelot combining rules.[54] The solute and solvent molecules are assumed to be rigid. Values of the potential parameters and molecular geometries are provided in Table I. The solute is a 12-site model of benzene, developed by Kumar and Maroncelli.[23] For acetonitrile we use the potential developed by Edwards *et al.*[55] In this representation the methyl group is modeled as a single interaction site, making the molecule effectively linear. For CO_2 we use the rigid version of the 3-site EPM2 model of Harris and Yung,[56] designed to match the liquid-vapor coexistence curve and critical properties of the real fluid. As noted in Sec. I these two solvent models have very similar masses, moments of inertia, and shapes as defined by molecular geometries and LJ σ_α parameters. In addition, the magnitudes of the charges are also similar; the primary difference in this regard is merely the *symmetry* of the charge distribution. To heighten the parallels between these two solvents we compare dynamics at the same molar volume, 52.18 cm^3/mol, and temperature, 298 K. In the case of CH_3CN, these conditions correspond to the normal liquid at atmospheric pressure. The CO_2 system is also a liquid, but close to its critical temperature. (The density is 1.81 ρ_c and the temperature 0.979 T_c.) By contrast, CH_3CN is much further from its critical state, being only at 0.543 T_c.

The MD simulations are performed on systems consisting of 1 solute and 252 solvent molecules. The solute is constrained to be stationary in order to focus attention solely on the solvent's contribution to the solvation response. The simulation is carried out at constant volume and energy with the system in a cubic cell with periodic boundary conditions and a spherical approximation to the Ewald summation,[57] using a time step of 4 fs. See Ref. 23 for further details. The results that we present are averages over 1 ns trajectories. In order to make a connection between the pure-solvent and solvation dynamics, we have also simulated pure CH_3CN and CO_2 systems containing 256 molecules at the same molar volume and temperature as the dilute solutions described above. The pure solvent TCFs are calculated by averaging over all molecules and over trajectories of about 16 ps.

We simulate hypothetical $S_0 \rightarrow S_1$ electronic transitions in the solute which alter the solute's partial charges by an amount Δq_α, such that the energy gap is of the form

$$\Delta E = \sum_\alpha \sum_{j=1}^{N} \sum_\beta \frac{\Delta q_\alpha q_\beta}{4\pi\epsilon_0 r_{0\alpha,j\beta}}, \tag{2.2}$$

where $r_{0\alpha,j\beta}$ is the distance between the solute (''0'') site α and site β on the jth solvent molecule. We consider four different transitions, all of them involving the partial charges on the carbon sites of the benzene solute. The charge perturbations, depicted in Fig. 1, entail different multipole orders (m), ranging from a monopolar (charge, $m=0$) to an octopolar ($m=3$) changes in the solute's charge distribution. $C(t)$ and $G(t)$ are calculated for systems in the presence the ground state solute. Since the ground state is the same in all cases, within the linear response approximation a single equilibrium simulation suffices to explore the dynamics of all of these different transitions.

The results that we report correspond to ΔE evaluated by using the minimum image convention and truncating interactions beyond $\frac{1}{2}$ of the simulation box length. The accuracy of this approximation was checked against evaluation of ΔE using real-space lattice sums.[58] No significant differences were found for any of the quantities whose values are reported here.

III. METHODS OF ANALYSIS AND DEFINITIONS OF QUANTITIES OF INTEREST

As noted above, our approach to the study of solvation mechanisms is based on the analysis of both $G(t)$ and $C(t)$. The questions that we aim to address concern the relative contributions of rotational and translational motions to solvation dynamics, the collective versus single-solvent molecule nature of the solvation response, and the dependence of these aspects of solvation dynamics on the multipolar character of ΔE and on solvent polarity. In this work we take the solute molecule to be stationary. This is, of course, an approximation, although not a drastic one, especially in the inertial regime of the solvation response. Chromophores such as C153 that are used in dynamic Stokes shift experi-

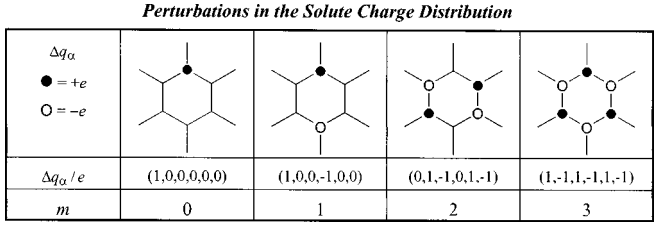

FIG. 1. The perturbations in solute charge distribution of a benzenelike solute corresponding to the different forms of ΔE used in this work. Values of the lowest multipole moment (m) of the perturbation are shown in the bottom row.

ments have much larger masses and moments of inertia than the solvents considered here, and their contribution to the solvation response in such solvents are therefore negligible, as has been confirmed in a recent MD study.[23]

Analysis of $G(t)$ allows us to identify the contributions of rotation, translation, and rotation-translation coupling to solvation dynamics.[22,24–26,44,47,48] As Steele pointed out,[49] it is relatively straightforward to identify contributions from molecular velocities corresponding to these different degrees of freedom to a velocity TCF associated with a collective variable such as ΔE. In the present case we consider a rigid, stationary solute in the presence of rigid, linear solvent molecules. The chain rule of differentiation allows us to separate $\Delta\dot{E}$ into contributions from solute-solvent electrostatic forces and torques on the one hand and solvent center-of-mass and angular velocities on the other. Identification of the rotational and translational components of $\Delta\dot{E}$ follows from this separation:

$$\Delta\dot{E}=\Delta\dot{E}^{\mathrm{trans}}+\Delta\dot{E}^{\mathrm{rot}}, \tag{3.1}$$

where

$$\Delta\dot{E}^{\mathrm{trans}}=\sum_{j=1}^{N}\sum_{\mu=x,y,z}\frac{\partial\Delta E}{\partial r_{j\mu}}\,\dot{r}_{j\mu}$$

and

$$\Delta\dot{E}^{\mathrm{rot}}=\sum_{j=0}^{N}\sum_{\mu=\theta,\phi}\frac{\partial\Delta E}{\partial r_{j\mu}}\,\dot{r}_{j\mu}. \tag{3.2}$$

The sums in these expressions are over N solvent molecules and over the three translational or two rotational coordinates of each solvent molecule j. As coordinates we use the set $r_{j\mu}=\{x_j,y_j,z_j,\theta_j,\phi_j\sin\theta_{j0}\}$, where the subscript ''0'' in $\sin\theta_{j0}$ indicates that this quantity is treated as time independent.[22,59] This breakdown of $\Delta\dot{E}$ yields the $G(t)$ in the form:

$$G(t)=G^{\mathrm{trans}}(t)+G^{\mathrm{cross}}(t)+G^{\mathrm{rot}}(t). \tag{3.3}$$

Single-solvent-molecule (s) and solvent-pair (p) contributions to $G(t)$ can also be identified from Eq. (3.2). They are obtained by constructing autocorrelation functions of the single-molecule contributions

$$\Delta\dot{E}_j^{\mathrm{trans}}=\sum_{\mu=x,y,z}\frac{\partial\Delta E}{\partial r_{j\mu}}\,\dot{r}_{j\mu}$$

and

$$\Delta\dot{E}_j^{\mathrm{rot}}=\sum_{\mu=\theta,\phi}\frac{\partial\Delta E}{\partial r_{j\mu}}\,\dot{r}_{j\mu}, \tag{3.4}$$

giving, for example,

$$G_s^{\mathrm{trans}}(t)=\sum_{j=1}^{N}\langle\Delta\dot{E}_j^{\mathrm{trans}}(0)\Delta\dot{E}_j^{\mathrm{trans}}(t)\rangle. \tag{3.5}$$

$G(t)$ can thus be expressed as a sum of single-solvent and solvent-pair velocity correlations,

$$G(t)=G_s(t)+G_p(t). \tag{3.6}$$

Since the velocities of different molecules and of different degrees of freedom in the same molecule are uncorrelated at $t=0$, $G_p(0)=0$, as are its translational and rotational components. [For the same reason $G^{\mathrm{cross}}(0)$ and its components are also zero.]

In analogy to the decomposition of $G(t)$, the solvation TCF itself, $C(t)$, can also be partitioned into single-solvent-molecule and solvent-pair terms:

$$C(t)=C_s(t)+C_p(t). \tag{3.7}$$

Writing ΔE as a sum of pairwise-additive solute-solvent interactions,

$$\Delta E=\sum_{j=1}^{N}\Delta w_{0j} \tag{3.8}$$

one finds

$$C_s(t)=\langle(\delta\Delta E)^2\rangle^{-1}\sum_{j=1}^{N}\langle\delta\Delta w_{0j}(0)\,\delta\Delta w_{0j}(t)\rangle, \tag{3.9}$$

etc., where $\delta\Delta w_{0j}=\Delta w_{0j}-\langle\Delta w_{0j}\rangle=\Delta w_{0j}-\langle\Delta E\rangle/N$.

There is a simple connection between $G_s(t)$ and $C_s(t)$ when the solute is immobile, namely

$$G_s(t)=-\langle(\delta\Delta E)^2\rangle\,\frac{d^2C_s(t)}{dt^2}, \tag{3.10}$$

and an analogous relation applies between the solvent-pair contributions

$$G_p(t)=-\langle(\delta\Delta E)^2\rangle\,\frac{d^2C_p(t)}{dt^2}. \tag{3.11}$$

An interesting consequence of this last relation and the fact that $G_p(0)=0$ is that $C_p(t)$ has zero initial curvature, i.e., $\ddot{C}_p(0)=0$, and it therefore does not contribute to the solvation frequency, $\omega_s=\sqrt{-\ddot{C}(0)}$, which characterizes the initial Gaussian-like decay of $C(t)$. Specifically, the short time expansion of $C(t)$ gives

$$C(t)\cong 1-\tfrac{1}{2}\omega_s^2t^2\cong\exp(-\tfrac{1}{2}\omega_s^2t^2). \tag{3.12}$$

Equation (3.10) thus implies that

$$\omega_s=\sqrt{G_s(0)/\langle(\delta\Delta E)^2\rangle}. \tag{3.13}$$

From this expression we see that ω_s consists of single-solvent-molecule dynamics scaled by the static intermolecular correlations contained in $\langle(\delta\Delta E)^2\rangle$.

Steele[49] described a cumulant expansion approach[60] to construct approximations to collective variable TCFs such as $C(t)$ in terms of static positional correlations and velocity TCFs. Here we use this method to derive approximate power-law relations between collective and single-molecule correlation functions in the spirit of Eq. (1.7). We will do so at two levels, first connecting $C(t)$ and $C_s(t)$ and then making further approximations needed to derive (1.7) and its extension for the case where translational contributions to $C(t)$ cannot be neglected.

To derive the first approximation for $C(t)$, we replace the exact relation Eq. (1.5) with the cumulant approximation,

$$C(t)=1-a(t)/\langle(\delta\Delta E)^2\rangle\cong\exp[-a(t)/\langle(\delta\Delta E)^2\rangle], \tag{3.14}$$

where

$$a(t)\equiv\int_0^t(t-\tau)G(\tau)d\tau. \tag{3.15}$$

A cumulant approximation can also be made for $C_s(t)$:

$$C_s(t)\cong C_s(0)\exp[-a_s(t)/\langle(\delta\Delta E)^2\rangle_s], \tag{3.16}$$

where

$$\langle\delta\Delta E^2\rangle_s\equiv\sum_{j=1}^{N}\langle(\delta\Delta w_{0j})^2\rangle, \tag{3.17a}$$

and

$$a_s(t)\equiv\int_0^t(t-\tau)G_s(\tau)d\tau. \tag{3.17b}$$

If we can assume that $a(t)\cong a_s(t)$, comparison of Eqs. (3.15) and (3.16) yields the power-law relationship

$$C(t)=[C_s(t)/C_s(0)]^{\alpha_s}, \tag{3.18}$$

where

$$\alpha_s=\langle(\delta\Delta E)^2\rangle_s/\langle(\delta\Delta E)^2\rangle=C_s(0). \tag{3.19}$$

Equation (3.18) provides the first approximate connection between the single-molecule and collective solvation responses. It should be accurate to the extent that the cumulant approximation is valid and $G(t)\cong G_s(t)$. We note that the equivalent of Eq. (3.19) for the ionic solute/rotation only case was derived in Ref. 51, where its physical content was discussed in some detail.

A second level of approximation is to connect $C(t)$ to simpler single molecule dynamics that are more readily interpreted than $C_s(t)$. To do so requires further approximations to $G(t)$. Denoting energy derivatives by

$$D_{j\mu}\equiv\frac{\partial\Delta E}{\partial r_{j\mu}}, \tag{3.20}$$

$G(t)$ can be expressed exactly as:

$$G(t)=\sum_{i,j}\sum_{\mu,\nu}\langle D_{i\mu}(0)\dot{r}_{i\mu}(0)D_{j\nu}(t)\dot{r}_{j\nu}(t)\rangle. \tag{3.21}$$

If we assume that both inter-molecular pair ($i\neq j$) terms (as above) and cross terms between different degrees of freedom on the same molecule ($\mu\neq\nu$) can be neglected, then

$$G(t)\cong\sum_{i}\sum_{\mu}\langle D_{i\mu}(0)D_{i\mu}(t)\dot{r}_{i\mu}(0)\dot{r}_{i\mu}(t)\rangle. \tag{3.22}$$

Finally, if we make the more serious assumptions that molecular velocities vary in time much more rapidly than molecular positions, and that positions and velocities are uncorrelated (all of which are strictly valid only at $t=0$) we have:

$$G(t)\cong\sum_{i}\sum_{\mu}\langle D_{i\mu}^2\rangle\langle\dot{r}_{i\mu}(0)\dot{r}_{i\mu}(t)\rangle$$
$$\cong G^{\rm rot}(0)\psi_{\rm rot}(t)+G^{\rm trans}(0)\psi_{\rm trans}(t), \tag{3.23}$$

where $\psi_{\rm rot}(t)$ and $\psi_{\rm trans}(t)$ are the normalized rotational and translational velocity TCFs of solvent molecules,

$$\psi_{\rm rot}(t)=\frac{I}{2k_BT}\sum_{\mu=\theta,\phi}\langle\dot{r}_{j\mu}(0)\dot{r}_{j\mu}(t)\rangle, \tag{3.24}$$

and

$$\psi_{\rm trans}(t)=\frac{M}{3k_BT}\sum_{\mu=x,y,z}\langle\dot{r}_{j\mu}(0)\dot{r}_{j\mu}(t)\rangle, \tag{3.25}$$

and where M and I are the solvent mass and moment of inertia. Note that for our choice of rotational coordinates, $\psi_{\rm rot}(t)$ is not precisely the molecular angular velocity autocorrelation function,[61]

$$\psi_{\omega}(t)=\frac{I}{2k_BT}\langle\omega_j(0)\cdot\omega_j(t)\rangle, \tag{3.26}$$

where $\omega_j=d\hat{\mathbf{u}}_j/dt$ and $\hat{\mathbf{u}}_j$ is a unit vector along the axis of the jth solvent molecule, but that it differs negligibly from $\psi_{\omega}(t)$ it under the conditions for which Eq. (3.23) is valid, i.e., when velocities decay considerably faster than the corresponding coordinates.

Equation (3.23) represents an approximation to $G(t)$ in terms of pure solvent dynamics in the form of single-molecule velocity TCFs $\psi_{\rm rot}(t)$ and $\psi_{\rm trans}(t)$ and the time-independent solute-solvent correlations $G^{\rm rot}(0)$ and $G^{\rm trans}(0)$. When this equation is valid, the cumulant approximation to $C(t)$ becomes

$$C(t)\cong\exp\{-[G^{\rm rot}(0)b_{\rm rot}(t)+G^{\rm trans}(0)b_{\rm trans}(t)]/\langle(\delta\Delta E)^2\rangle\}, \tag{3.27}$$

where

$$b_{\rm rot}(t)=\int_0^t(t-\tau)\psi_{\rm rot}(\tau)d\tau \tag{3.28}$$

and $b_{\rm trans}(t)$ is defined in an analogous way. To arrive at Eq. (1.7), we note that the single-molecule orientational TCF of order l can also be obtained in terms of a first-order cumulant approximation[62]

$$C_l(t)=\langle P_l[\hat{\mathbf{u}}_j(0)\cdot\hat{\mathbf{u}}_j(t)]\rangle\cong\exp\left[-\frac{l(l+1)k_BT}{I}b_{\rm rot}(t)\right], \tag{3.29}$$

where P_t is the Legendre polynomial of order l and where have assumed $\psi_{\omega}(t)\cong\psi_{\rm rot}(t)$. Comparison of Eqs. (3.27) and (3.29) indicates that Eq. (1.7) results from the further assumption that translational dynamics make a negligible contribution to $C(t)$, i.e., that $G^{\rm trans}(0)\ll G^{\rm rot}(0)$. In this case, one finds

$$C(t)\cong[C_l(t)]^{\alpha_l}\ \text{ with }\ \alpha_l=\frac{IG^{\rm rot}(0)}{l(l+1)k_BT\langle\delta\Delta E^2\rangle}, \tag{3.30}$$

where we have used the fact that $\langle(\dot{r}_{j\mu})^2\rangle=k_BT/I$ for $\mu=\theta,\phi$.

When the translational contribution to Eq. (3.27) is not negligible, the relevant solvent dynamics can, at long times, be related to translational diffusion of solvent molecules. Specifically,

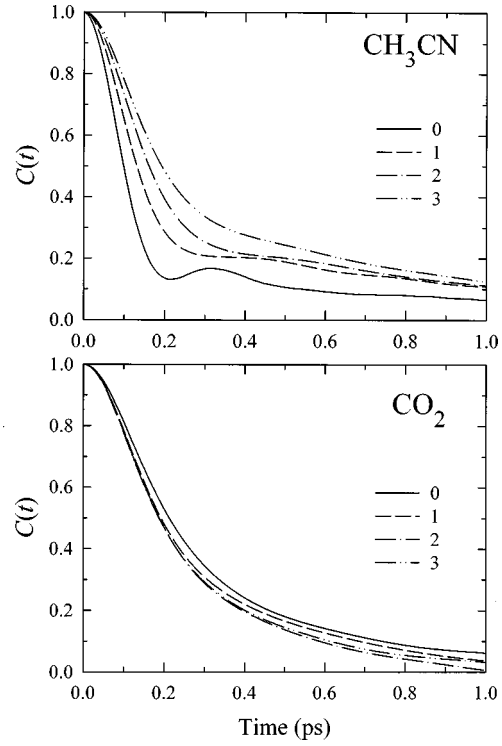

FIG. 2. Solvation time correlation functions $C(t)$ for different forms of ΔE in CH_3CN (top panel), CO_2 (bottom panel). Different line styles correspond to $m=0$ (full line), 1 (dashed line), 2 (dash-dotted line), and 3 (dash-double dotted line).

$$b_{\mathrm{trans}}(t)=\frac{k_BT}{6M}\langle[\mathbf{r}_j(t)-\mathbf{r}_j(0)]^2\rangle, \tag{3.31}$$

where $\mathbf{r}_j$ is the position of the center-of-mass of the jth solvent molecule. At long times

$$\lim_{t\to\infty} b_{\mathrm{trans}}(t)/t=\frac{k_BT}{M}D. \tag{3.32}$$

where D is the solvent translational diffusion coefficient. Several theories of electrostatic solvation dynamics that include the contribution of solvent translational diffusion have been developed.[63–66] Our formalism allows us to determine the contribution of translation to $C(t)$ at all time scales, including short times for which Eq. (3.32) is invalid, and relate it approximately to pure solvent dynamics using the solvent center-of-mass velocity TCF as basic input. It also clarifies under which conditions translation becomes an important contributor to solvation dynamics.

We remind the reader here that Eqs. (3.18) and (3.27) which relate $C(t)$, respectively, to single-solvent and pure-solvent dynamics were derived by assuming that the solute is stationary. Our MD simulations correspond to these conditions. For a moving solute, $G(t)$ would also contain contributions from solute $(j=0)$ center-of-mass and angular velocities. Equation (3.23), would then include, in addition to the solvent functions $\psi_{\mathrm{rot}}(t)$ and $\psi_{\mathrm{trans}}(t)$, the rotational and translational velocity TCFs for the solute at infinite dilution

TABLE II. Summary of static and dynamic properties.

A. Total system values

Solute Δq_α	m	$\langle\delta\Delta E^2\rangle$ 10^{-4} au	$G(0)$ 10^{-12} au	$G^{\mathrm{rot}}(0)$ 10^{-12} au	$G^{\mathrm{trans}}(0)$ 10^{-12} au	f^{trans} %	ω_s ps^{-1}	ω_s^{rot} ps^{-1}	$\omega_s^{\mathrm{trans}}$ ps^{-1}
				Acetonitrile					
(+00000)	0	1.84	14.9	13.7	1.22	8.2	11.8	11.3	3.4
(+00−00)	1	1.04	5.81	4.68	1.13	19.5	9.8	8.8	4.3
(0+−0+−)	2	0.300	1.25	0.856	0.393	31.5	8.4	7.0	4.7
(+−+−+−)	3	0.084	0.288	0.168	0.118	41.4	7.7	5.8	4.9
				Carbon Dioxide					
(+00000)	0	0.344	0.936	0.829	0.105	11.2	6.8	6.4	2.3
(+00−00)	1	0.354	1.12	0.959	0.172	15.2	7.4	6.8	2.9
(0+−0+−)	2	0.138	0.453	0.348	0.104	23.0	7.5	6.6	3.6
(+−+−+−)	3	0.045	0.151	0.103	0.048	31.8	7.6	6.3	4.3

B. Single-solvent-molecule contributions

Solute Δq_α	m	$\langle\delta\Delta E^2\rangle_s$ 10^{-4} au	α_s	$G_s(0)$ 10^{-12} au	$G_s^{\mathrm{rot}}(0)$ 10^{-12} au	$G_s^{\mathrm{trans}}(0)$ 10^{-12} au	f_s^{trans} %	$\omega_{s,s}$ ps^{-1}	$\omega_{s,s}^{\mathrm{rot}}$ ps^{-1}	$\omega_{s,s}^{\mathrm{trans}}$ ps^{-1}
					Acetonitrile					
(+00000)	0	17.0	9.26	14.7	13.5	1.22	8.3	3.8	3.7	1.1
(+00−00)	1	6.00	5.75	5.72	4.60	1.12	19.5	4.0	3.6	1.8
(0+−0+−)	2	1.07	3.55	1.23	0.841	0.387	31.5	4.4	3.7	2.5
(+−+−+−)	3	0.192	2.29	0.282	0.167	0.115	40.8	5.0	3.8	3.2
					Carbon Dioxide					
(+00000)	0	0.436	1.27	0.928	0.822	0.105	11.3	6.0	5.7	2.0
(+00−00)	1	0.399	1.13	1.126	0.956	0.171	15.2	7.0	6.4	2.7
(0+−0+−)	2	0.158	1.14	0.466	0.359	0.105	22.7	7.1	6.2	3.4
(+−+−+−)	3	0.051	1.14	0.155	0.106	0.048	31.3	7.2	6.0	4.0

in this solvent. However, for the large chromophores typically used in solvation dynamics experiments, $M_0 \gg M$ and $I_0 \gg I$. Consequently, solute dynamics, while straightforward to include into approximate and exact expressions for $C(t)$, have little impact on it in the cases of most interest here.[23]

IV. RESULTS AND DISCUSSION

A. Basic features of the solvation response

The object of ultimate interest in this work is the solvation response function $S(t)$, or equivalently, the solvation TCF, $C(t)$. We therefore begin by describing the basic features of $C(t)$ and its dependence on solute perturbation and solvent polarity. Figure 2 contains the basic results of the simulations: $C(t)$ functions for the four benzene perturbations, corresponding to $m=0$, 1, 2, and 3, in CH_3CN and CO_2. As can be seen from Fig. 2, very different m-dependence is observed for the solvation response in these two solvents. The trend displayed here in CH_3CN had previously been reported by Kumar and Maroncelli,[23] who also found the same behavior in methanol (cf. Fig. 11 of Ref. 23). In such highly polar solvents the general trend appears to be that $C(t)$ decays appreciably more slowly as m increases. By contrast, in the nondipolar solvent CO_2, solvation dynamics has a much weaker m-dependence and shows predominantly the *opposite* trend with increasing m: The slowest decay of $C(t)$ occurs for $m=0$ and the next slowest for $m=1$. The $m=2$ and $m=3$ solutes exhibit approximately the same solvation response with the latter slightly slower at $t>0.5$ ps. Comparing the results for the two solvents to each other, we also see that solvation dynamics at low m values is significantly faster in CH_3CN than in CO_2.

Although our main interest is in the dynamics of solvation, it is worth digressing momentarily to examine the relative magnitudes of the solvation energies involved here. These energies are reflected in the $t=0$ amplitudes of the solvation TCFs, $\langle \delta\Delta E^2 \rangle$, listed in Table IIA. Such fluctuation magnitudes are proportional to the linear response estimates for the solvation energy change that would accompany the solute charge perturbations indicated in Fig. 1. From the data in Table IIA one finds that the solvation energies in both solvents decrease markedly between the $m=0$ and $m=3$ solutes, as expected. The solvation of an ionic species is much more efficient in acetonitrile than in CO_2: $\langle \delta\Delta E^2 \rangle$ for the $m=0$ perturbation is about five times greater in the dipolar solvent acetonitrile than it is in the nondipolar solvent CO_2. However, this disparity decreases as the multipolar order of the perturbation increases (and thus the range of the interactions decreases.) It is interesting to note that for the dipolar ($m=1$) perturbation the simulated difference in electrostatic solvation energies is about a factor of 3, which is comparable to what is observed experimentally[42] for the predominantly dipolar $S_0 \rightarrow S_1$ transition in C153: $[\overline{\Delta E(0)} - \overline{\Delta E(\infty)}]_{CH_3CN} / [\overline{\Delta E(0)} - \overline{\Delta E(\infty)}]_{CO_2} = 3.5 \pm 0.6$. This similarity, along with more extensive evidence presented in Ref. 42, demonstrates that even in nondipolar solvents such as CO_2 the primary mechanism of solvation is the same as in highly polar solvents like CH_3CN. Thus, as far as solvation energies go, there are quantitative but not qualitative differences between these two solvents.

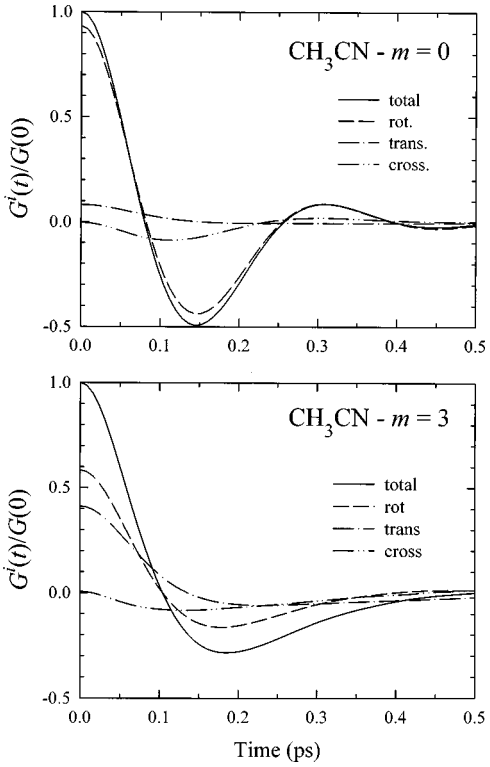

FIG. 3. Decomposition of the normalized solvation velocity time correlation functions in CH_3CN into rotational (dashed line), translational (dash-dotted line), and rotation-translation cross-correlation (dash-double dotted) components. Results for the $m=0$ perturbation are shown in the top and for $m=3$ in the bottom panel.

Returning now to dynamics, we note that compared to these energetics, differences between the dynamics in these two solvents are much more dramatic. In spite of the similarities in size, shape, and inertial characteristics of the two solvents, there are *qualitative* differences in the ways that polar and nondipolar solvents respond to different changes in the solute charge distribution. In order to explain the solute m- and solvent dependence displayed in Fig. 2, we have performed additional calculations designed to reveal several aspects of the molecular mechanisms of solvation dynamics. In the following section we first examine how the contributions of solvent rotational and translational motions to $C(t)$ vary with m. As explained in Sec. III, these contributions can be identified in the solvation velocity TCF, $G(t)$. The question of the collective nature of the solvent response is then addressed in part C. Finally, in part D we test the utility of approximate connections between $C(t)$ and single-solvent-molecule correlation functions derived in Sec. III.

B. Contributions of rotational and translational dynamics to the solvent response

Information on the relative contributions of solvent-molecule rotation and translation to solvation dynamics is accessible through $G(t)$, as Eq. (3.3) indicates. The results of decomposing $G(t)$ into $G^{\mathrm{trans}}(t)$, $G^{\mathrm{cross}}(t)$, and $G^{\mathrm{rot}}(t)$ for the $m=0$ and $m=3$ perturbations are shown in

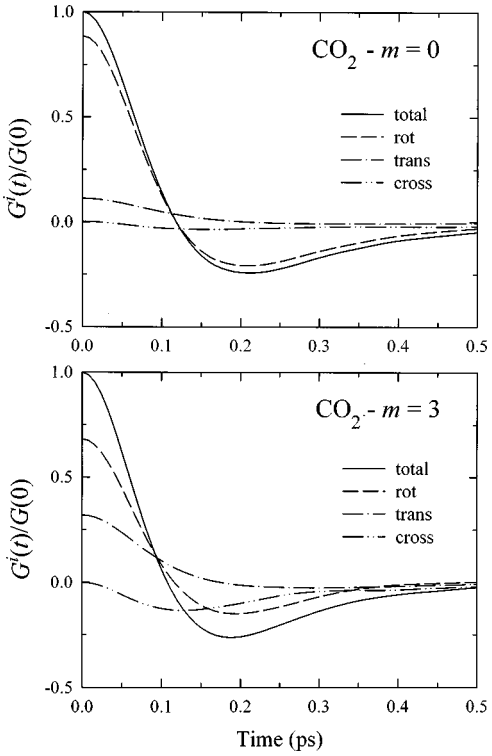

FIG. 4. Same as Fig. 3, but for solvation dynamics in CO_2.

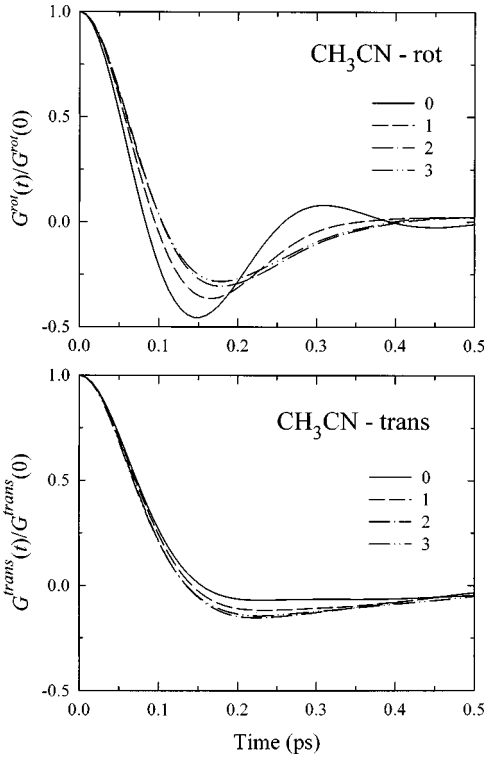

FIG. 5. Comparison of the normalized rotational (top panel) and translational (bottom panel) componenets of the solvation velocity time correlation function in CH_3CN for different m values. Different line styles indicate different m values as in Fig. 2.

Figs. 3 (CH_3CN) and 4 (CO_2). In both solvents $G^{\mathrm{rot}}(t)$ clearly dominates for $m=0$, but its importance diminishes considerably for $m=3$. This trend might be anticipated based on the fact that the effective solute-solvent interaction range diminishes with increasing m: The leading term in the expansion of $\Delta\omega_{0j}$, the contribution to ΔE from the jth solvent molecule, in inverse powers of intermolecular center-of-mass distance r_{0j} is given by

$$\Delta\omega_{0j}\sim a_n(\Omega_0,\hat{\mathbf{u}}_j,\hat{\mathbf{r}}_{0j})/r_{0j}^{n+m}, \tag{4.1}$$

where a_n is a rotationally invariant function of the solute orientation Ω_0, the jth solvent molecule orientation $\hat{\mathbf{u}}_j$, and $\hat{\mathbf{r}}_{0j}=\mathbf{r}_{0j}/r_{0j}$, the unit vector along the solute-solvent center-of-mass separation. n is related to the order of the leading solvent multipole, $n=2$ for CH_3CN, and $n=3$ for CO_2. Since $\Delta\omega_{0j}$ becomes proportional to a higher inverse power of r_{0j} with increasing m, it varies more rapidly with a given change in translational coordinates as m increases.

Judging from the small magnitude of $G^{\mathrm{cross}}(t)$, translation-rotation coupling does not play a large role in solvation dynamics. Its relative importance increases slightly with increasing m. This fact is consistent with the expectation that if there is any rotation-translation coupling present in the system, its contribution to a particular observable will become greater when the contributions of rotation and translation to this observable are nearly equal. In the present case, this near equality is reached at higher m values.

Figures 5 and 6 depict the m-dependence of the normalized functions $G^{\mathrm{rot}}(t)$ and $G^{\mathrm{trans}}(t)$ in the two solvents. As Eqs. (3.2) indicate, there are two sources of m-dependence of these functions: One is direct and comes from the m-dependence of the electrostatic force or torque $D_{j\mu}$ [Eq. (3.20)] and the other indirect and related to the m-dependence of the solvent-pair contributions to $G^{\mathrm{rot}}(t)$ and $G^{\mathrm{trans}}(t)$.

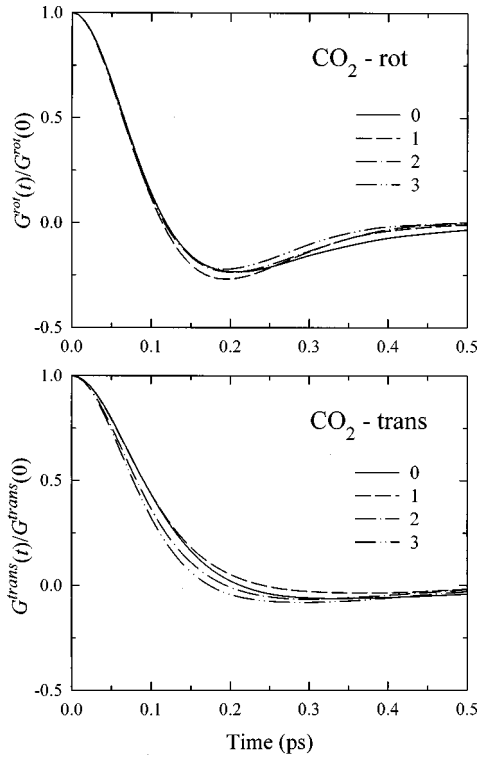

FIG. 6. Same as Fig. 5, but for solvation dynamics in CO_2.

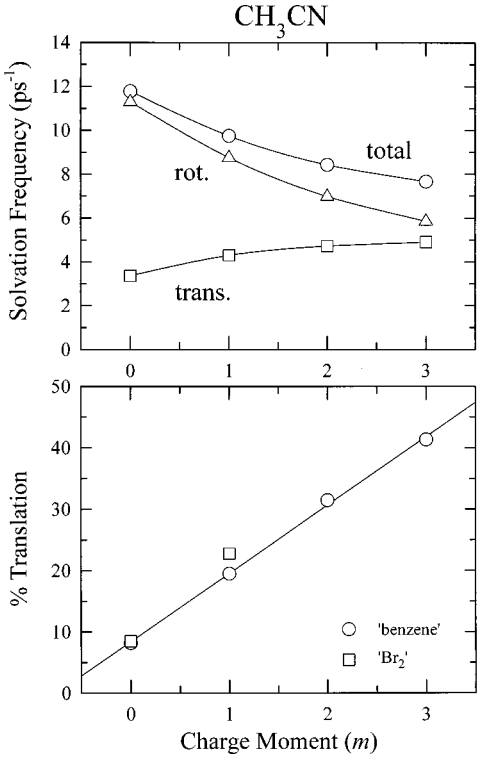

FIG. 7. Dependence of the solvation frequency ω_s on the perturbation moment m in CH_3CN. The top panel depicts ω_2 (circles), and its rotational (ω_s^{rot}; triangles) and translational (ω_s^{trans}; squares) components. The bottom panel depicts f^{trans}, the contribution of translational motion to ω_s^2 for a benzenelike (hollow circles) and brominelike (gray squares) solutes. The least squares fit of the benzenelike solute data to a straight line is also shown.

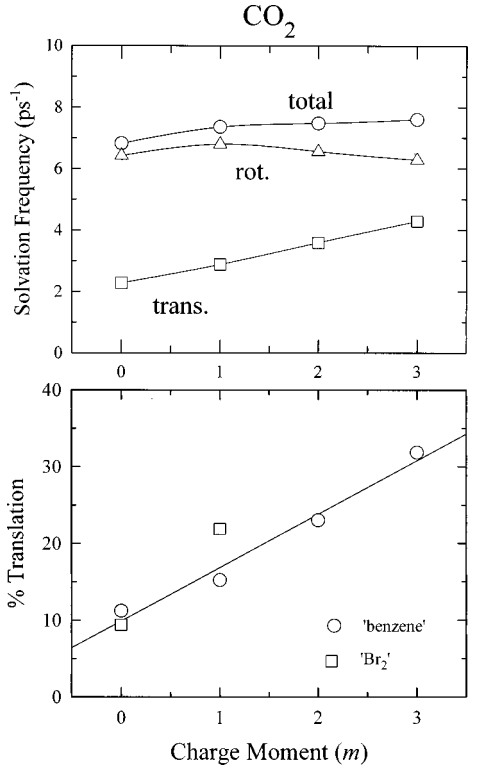

FIG. 8. Same as Fig. 7, but for solvation dynamics in CO_2.

$G^{trans}(t)$ is weakly m-dependent in both solvents and its initial decay rate increases with increasing m. This rate increase is consistent with the fact that $D_{j\mu}$ $(\mu=x,y,z)$ becomes a more rapidly varying function of the solute-solvent center-of-mass separation r_{0j} as m increases. Specifically, according to Eqs. (3.9) and (4.1), the leading term in $D_{j\mu} \propto r_{0j}^{-(m+n+1)}$ for $\mu=x,y,z$.

The m-dependence of $G^{rot}(t)$ is very different in the two solvents: In CH_3CN, $G^{rot}(t)$ exhibits significantly faster initial decay and a deeper, more pronounced negative recoil at smaller m. In CO_2, on the other hand, $G^{rot}(t)$ has almost no m-dependence. As we shall see, the source of this difference can be traced to intermolecular angular velocity correlations, which are more pronounced in the case of CH_3CN. They have a stronger effect on the $G^{rot}(t)$ for small m, due to the fact that $D_{j\mu}$ is then longer ranged, sampling intermolecular correlations involving a larger number of solvent molecules.

The short time dynamics of solvation can be characterized by the solvation frequency, ω_s, given by Eq. (3.13). By virtue of the lack of correlation at $t=0$ between velocities for different degrees of freedom

$$\omega_s^2=(\omega_s^{rot})^2+(\omega_s^{trans})^2. \tag{4.2}$$

Results for the solvation frequency and its components are shown in Figs. 7 and 8 for the CH_3CN and CO_2 solvents, respectively. The top panels of these figures depict the dependence of ω_s, ω_s^{rot}, and ω_s^{trans} on m. The bottom panels show f^{trans}, the fractional contribution of translational dynamics to ω_s^2,

$$f^{trans}=G^{trans}(0)/G(0)=(\omega_s^{trans})^2/\omega_s^2. \tag{4.3}$$

All of these quantities are also provided in numerical form in Table II.

From Figs. 7 and 8 we see that in CH_3CN, ω_s decreases substantially with increasing m, while in CO_2 it increases slightly. This difference in behavior can be largely traced to the different m-dependence of ω_s^{rot} in the two solvents: In CH_3CN ω_s^{rot} decreases rapidly with increasing m, while in CO_2 it shows essentially no m-dependence. In both solvents, ω_s^{trans} increases slowly as m increases. In CO_2 the m-dependence of ω_s largely follows ω_s^{trans}, whereas in CH_3CN the rapid decrease in ω_s^{rot} wins out over the slow increase in ω_s^{trans}. The overall result is that the solvation frequencies in the two liquids, which start off very different at $m=0$ become nearly the same at $m=3$.

The contribution of translational motion, f^{trans}, increases steadily with m in both solvents. The variation is somewhat greater in CH_3CN (8%–41%) compared to CO_2 (11%–32%) as m varies from 0 to 3. This sort of trend was predicted by Ladanyi and Stratt[25] who related it to the decrease in the effective range of ΔE with increasing m. As noted in connection with Figs. 3 and 4, the decrease in the effective range of multipolar interactions also leads to a larger translational contribution to solvation dynamics at longer times. In CH_3CN, f^{trans} is nearly linear in m and insensitive to solute type: The results for a brominelike diatomic,[22,25,26] also shown in Fig. 7, are very similar to

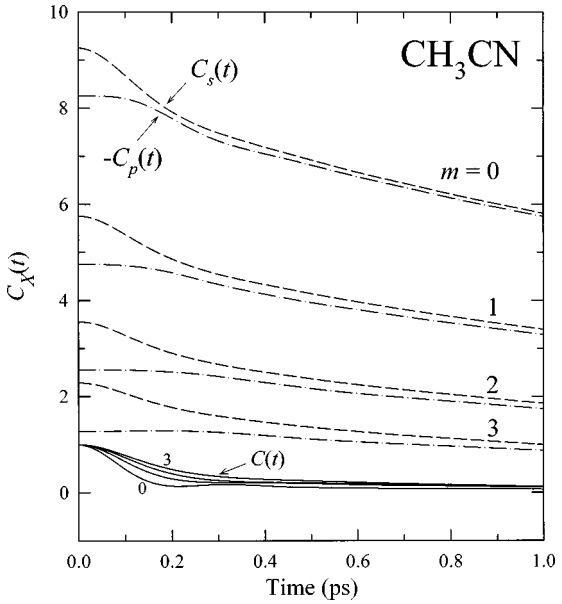

FIG. 9. Decomposition of the solvation TCF $C(t)$ (full line) into its single-solvent $C_s(t)$ (dashed line) and pair $C_p(t)$ components in the CH_3CN solvent for $m=0$, 1, 2, and 3. Note that $-C_p(t)$ (dash-dotted line), the negative of the pair component, is shown.

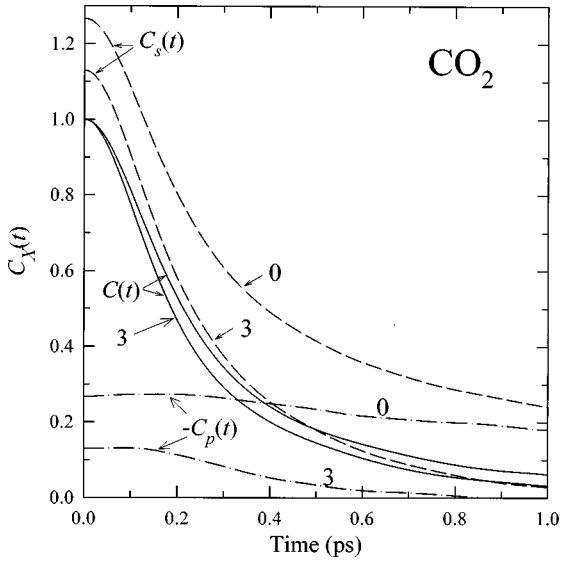

FIG. 10. Same as Fig. 9, but for solvation dynamics in CO_2. In this case only the $m=0$ and $m=3$ data are plotted.

those for benzene. In CO_2, f^{trans} is also approximately linear in m, but its values show more scatter and stronger dependence on the solute shape. However, even in this solvent f^{trans} correlates quite well with the multipolar character of ΔE.

Recalling that $\omega_s^2 = G(0)/\langle \delta\Delta E^2 \rangle$, further insights into the static ($\langle \delta\Delta E^2 \rangle$), and dynamic ($G(0)$) factors influencing ω_s can be obtained from the data in Table IIA. The tabulated results indicate that both $\langle \delta\Delta E^2 \rangle$ and $G(0)$ exhibit a strong m-dependence in CH_3CN, both decreasing substantially with increasing m: $\langle \delta\Delta E^2 \rangle$ by a factor of 22 and $G(0)$ by a factor of 52 as m increases from 0 to 3. In CO_2 both quantities exhibit a weaker m-dependence. In going from $m=0$ to 1 they increase slightly and then decrease in going from $m=1$ to 3: $\langle \delta\Delta E^2 \rangle$ by a factor of 7.8 and $G(0)$ by a factor of 7.4. At $m=0$, $\langle \delta\Delta E^2 \rangle$ and $G(0)$ in CO_2 are an order of magnitude smaller than in CH_3CN, but because of their weaker m-dependence, both quantities are less than a factor of 2 smaller than their CH_3CN counterparts for $m=3$. Thus both static and dynamic factors influencing ω_s exhibit weaker dependence on solvent polarity for higher multipole perturbations in the solute charge distribution.

C. How collective is the solvent response?

Since the form of ΔE we are considering is a sum of solute-solvent electrostatic interactions and is therefore pairwise additive [Eqs. (2.2) and (3.8)], the solvation TCF $C(t)$ can be separated into single-solvent-molecule $C_s(t)$ and solvent-pair $C_p(t)$ components. The latter function measures the extent to which solvent-solvent correlations contribute to solvation dynamics. Figures 9 and 10 illustrate this separation for solvation in CH_3CN and CO_2, respectively. Since $C_p(t)$ is negative, we plot $-C_p(t)$ to make the comparison of its time evolution and that of $C_s(t)$ easier.

Figure 9 shows that solvation dynamics in CH_3CN is *highly collective*. At all m values, $C_p(t)$ makes a substantial contribution to $C(t)$. Since it is negative, its effect is to partially cancel the contribution of $C_s(t)$. The extent of this cancellation increases with decreasing m and for $m=0$ becomes nearly complete. The resulting $C(t)$ relaxes much more rapidly than either $C_s(t)$ or $C_p(t)$ and the amplitude of the response is almost *an order of magnitude smaller*. The m-dependence of $C_p(t)$ and its cancellation of $C_s(t)$ is the reason why $C(t)$ decays faster at smaller m, even though $C_s(t)$ decays more rapidly as m increases.

Figure 10 shows that the situation is very different in CO_2. In this case, $-C_p(t) \ll C_s(t)$ and the extent of the cancellation of $C_s(t)$ by $C_p(t)$ is much smaller. As in CH_3CN, the contribution of $C_p(t)$ diminishes with increasing m, but in the CO_2 case it is quite small even at $m=0$. Solvation dynamics is largely determined by the single-molecule solvent response. Faster decay of $C(t)$ at larger m observed for this solvent follows the m-dependence of the decay rate of $C_s(t)$.

The phenomenon of partial cancellation of contributions to collective TCFs from correlations of different numbers of molecules seems quite widespread in dense fluid systems. In the context of solvation, cancellation effects of ΔE by $C_p(t)$ had been observed previously[26] for electrostatic $C_p(t)$ fluctuations for diatomic solutes in acetonitrile and CO_2 and for nonelectrostatic solute-solvent potential fluctuations in atomic solvents.[67] There are also numerous examples involving TCFs of dynamical variables observable in absorption, light scattering, and nonlinear optical spectroscopies in pure dense fluids.[68] Especially relevant to electrostatic solvation are charge density fluctuations in the pure solvent,[69] which are related to the wave vector (k) dependent longitudinal dielectric permittivity.[55,70–74] In polar liquids at small k dramatic cancellation between single-molecule and pair contributions to the charge density fluctuation TCF is observed,[75,76] quite similar to the $C_s(t) - C_p(t)$ cancellation

presented here for low-m solvation dynamics in acetonitrile.

Table II contains further information about the relation between single-solvent-molecule and collective aspects of solvation. One of the quantities listed is α_s [cf. Eq. (3.19)] which provides a measure of how collective static solvation is. As illustrated in Fig. 9, a large value of α_s $[=C_s(0)]$ indicates that equilibrium solvation is highly collective, i.e., that $C_p(0)$ is a major contributor to $C(0)$. The values of α_s and $\langle \delta\Delta E^2\rangle$, the single-molecule solvent contribution to $\langle \delta\Delta E^2\rangle$, for solvation in CH_3CN and CO_2 are listed in part B of Table II. As anticipated from Figs. 9 and 10, α_s values in CH_3CN are considerably larger than in CO_2. In CH_3CN they are also much more strongly m-dependent, decreasing from 9.3 to 2.3 as m increases from 0 to 3. In CO_2 α_s ranges from 1.13 to 1.27, indicating that solvent-solvent correlations contribute very little to static solvation in this solvent.

Information about the short time dynamics of the single-molecule solvent response is also available from Table IIB, in the form of the single-solvent-molecule solvation frequency,

$$\omega_{s,s}=[G_s(0)/\langle \delta\Delta E^2\rangle_s]^{1/2}, \tag{4.4}$$

which characterizes the initial curvature of $C_s(t)$, i.e., $C_s(t)/C_s(0)=1-\frac{1}{2}\omega_{s,s}^2t^2+O(t^4)$. For both CH_3CN and CO_2 $\omega_{s,s}$ increases with increasing m, signaling faster initial single-molecule solvent response as m increases. Note that, at any given m, $\omega_{s,s}$ is larger in CO_2 than in CH_3CN, in contrast to the collective solvation frequency ω_s (cf. Table IIA) which is always larger in CH_3CN. In CH_3CN $\omega_{s,s}$ and ω_s have the *opposite* m-dependence and differ markedly in magnitude, especially at low m, where $\omega_{s,s}$ is much smaller than ω_s, indicating that the initial decay of $C(t)$ is much faster than the decay of $C_s(t)$. In CO_2, by contrast, $\omega_{s,s}$ and ω_s have the same m-dependence and differ very little in magnitude. Thus, just like in the case of static solvation, the short time solvation response in the two solvents differs markedly because of the more collective nature of solvation in acetonitrile. This difference is most pronounced at $m=0$ because ΔE then has the longest range and thus the largest number of solvent molecules participate significantly in solvation dynamics of a given solute. As a result, solvent–solvent correlations, which are evidently much stronger in a polar liquid, make a larger contribution to $\langle \delta\Delta E^2\rangle$ and $C(t)$.

Parts A and B of Table II include, respectively, the $t=0$ values of the total, $G(0)$, and single-solvent, $G_s(0)$, solvation velocity TCFs. As noted in Sec. III, because velocities for different degrees of freedom are uncorrelated at $t=0$, $G(0)=G_s(0)$ and their rotational and translational components should be equal as well. In the present work $G(0)$ and $G_s(0)$ were calculated from independent simulations. The small differences between them, as well as between $G^{\rm rot}(0)$ and $G_s^{\rm rot}(0)$ and between $G^{\rm trans}(0)$ and $G_s^{\rm trans}(0)$, provide a measure of the accuracy of our results.

D. Approximations to $C(t)$ in terms of single-molecule and pure-solvent dynamics

For ΔE corresponding to ionic $(m=0)$ perturbations in the solute-solvent potential, Maroncelli *et al.*[51] proposed the approximate connection [Eq. (1.7)] between the solvation response and the solvent dipole orientational TCF, $C_1(t)$: $C(t)\cong\{C_1(t)\}^{\alpha_1}$. A number of studies have shown that for such perturbations Eq. (1.7) provides a surprisingly accurate estimate of $C(t)$ in polar liquids.[35,47,51,77] The results presented in part B of this section provide a partial explanation for the success of this approximation. As we have shown, the solvent response to $m=0$ perturbations in solute-solvent electrostatic interactions is indeed predominantly through rotational motions of solvent molecules, such that neglect of the small translational contribution to $C(t)$ is justified. Neglecting translation would, however, be less reasonable at higher m, where translational contributions become progressively more important, as Figs. 3, 4, 7, and 8 indicate. We therefore explore two approximations to $C(t)$ that are similar in spirit to Eq. (1.7) but which include the effects of both translational and rotational dynamics.

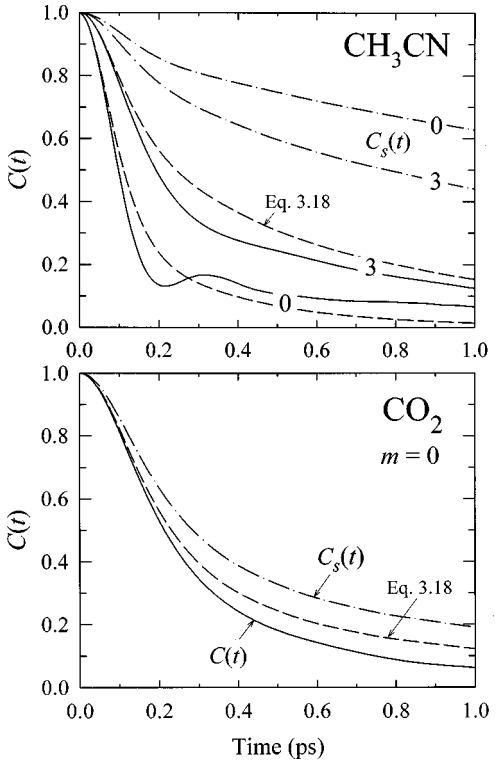

FIG. 11. Comparison of the exact solvation TCF $C(t)$ (full lines) with the approximate power-law relation, Eq. (3.18) (dashed lines). The dash-dotted lines depict the normalized single-molecule contributions $C_s(t)/C_s(0)$. The results for solvation in CH_3CN corresponding to $m=0$ and $m=3$ are in the top panel. The $m=0$ data for solvation in CO_2 are in the bottom panel.

The first approximation is Eq. (3.18), which connects $C(t)$ to the single-molecule solvent response: $C(t)=[C_s(t)/C_s(0)]^{\alpha_s}$. The accuracy of this power-law relationship for both CH_3CN and CO_2 is illustrated in Fig. 11. The top panel shows that Eq. (3.18) provides a good approximation to the short time solvation dynamics in CH_3CN. Much of the Gaussian-like initial decay of $C(t)$ is correctly predicted, as is the overall timescale of solvation response. Although the agreement is not perfect (for reasons to be discussed shortly) it is quite remarkable in view of the fact that α_s values (cf., Table IIB) are very different from each other for the $m=0$ and $m=3$ perturbations displayed. Figure 11 also shows more clearly than did Fig. 9 that $C_s(t)/C_s(0)$

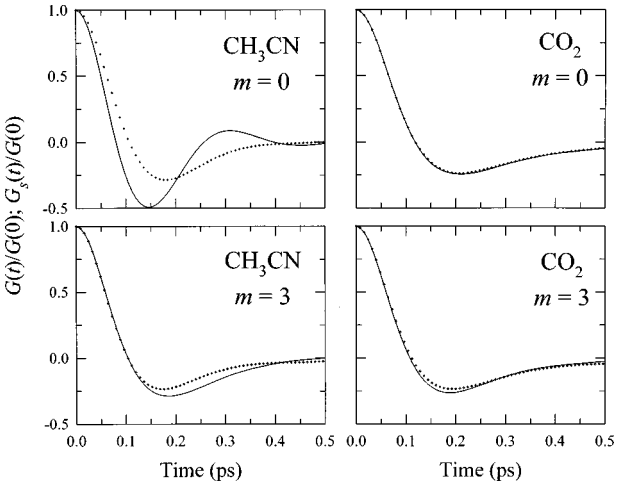

FIG. 12. Comparison of normalized solvation velocity TCFs ($G(t)/G(0)$; solid curves) with their single-molecule components ($G_s(t)/G(0)$; crosses) for $m=0$ and $m=3$ perturbations in CH_3CN and CO_2 solvents.

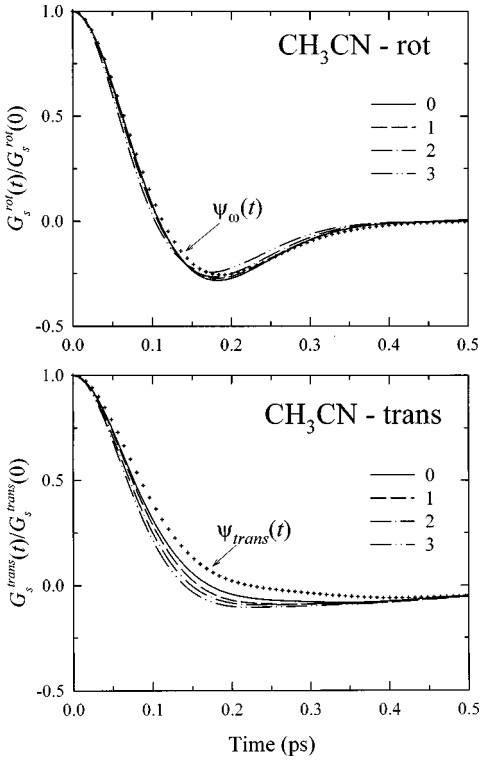

FIG. 13. Comparison of the normalized single-solvent contributions to the solvation velocity TCF in CH_3CN and pure-solvent velocity autocorrelations (crosses). The top panel depicts $G_s^{\mathrm{rot}}(t)/G_s^{\mathrm{rot}}(0)$ and $\psi_\omega(t)$, the solvent angular velocity TCF, and the bottom panel $G_s^{\mathrm{trans}}(t)/G_s^{\mathrm{trans}}(0)$ and the solvent center-of-mass velocity TCF, $\psi_{\mathrm{trans}}(t)$. Different line styles correspond to $m=0$ (full line), 1 (dashed line), 2 (dash-dotted line), and 3 (dash-double dotted line).

decays faster at higher m values, in spite of the fact that the corresponding collective $C(t)$ functions decay more slowly. Equation (3.18) correctly predicts this trend.

Equation (3.18) also provides a good approximation in the case of CO_2, as can be seen in the bottom panel of Fig. 11. These data shown here represent a test using the $m=0$ form of ΔE, which happens to exhibit the poorest agreement between the exact and approximate $C(t)$ functions in the case of CO_2. As can be seen from Fig. 11, even in this worst case, Eq. (3.18) works reasonably well. Good agreement here is hardly surprising, given that α_s is only 1.27, and raising $C_s(t)/C_s(0)$ to this near-unit power does not significantly modify its decay rate. Nevertheless, Eq. (3.18) correctly predicts the slight increase in decay rate of $C(t)$ compared to $C_s(t)$ here and the even smaller rate increases in the higher-m perturbations.

Given the apparent success of this simple approximation to $C(t)$, it is instructive to examine the approximations that underlie it. Equation (3.18) is exact at sufficiently short times. Thereafter, departures can arise from two sources: dynamical correlations between molecules, i.e., intermolecular velocity correlations that may be important in $G(t)$, but neglected in approximating it by $G_s(t)$, and the inaccuracy of the first-order cumulant approximation employed [Eq. (3.14)]. The relative importance of these two approximations can be judged from the comparisons of $G(t)$ and $G_s(t)$ provided in Fig. 12.

Consider the CO_2 results in Fig. 12 first. In CO_2, especially in the case of the $m=0$ perturbation, there is almost no observable distinction between $G_s(t)$ and $G(t)$. Thus, dynamical intermolecular correlations appear to be of no consequence to the solvation response in CO_2. Use of the single-solvent-molecule function $G_s(t)$ should therefore lead negligible error. In fact, the near-perfect agreement displayed in the case of the $m=0$ perturbation in CO_2 allows for some assessment of the effect of the cumulant approximation on $C(t)$ prediction. If one substitutes $G_s(t)$ for $G(t)$ into the exact expression for $C(t)$ [Eq. (1.5)], much better match between the exact and approximate solvation TCFs is obtained than is displayed in Fig. 11. Thus, in this particular example, we can attribute the majority of the deviation between $C(t)$ and $\{C_s(t)/C_s(0)\}^{\alpha_s}$ to inaccuracies in the cumulant approximation. The same cannot be said in the case of CH_3CN. In this strongly polar solvent, Fig. 12 reveals that dynamical intermolecular correlations are far from negligible. Here differences between $G_s(t)$ and $G(t)$ are considerably larger than in CO_2 for all m values, with these differences being greatest at small m.

Insight into the origins of the dynamical correlations present in CH_3CN can be obtained by comparing the rotational and translational components of $G_s(t)$, shown in Figs. 13 and 14, with their $G(t)$ counterparts already presented in Figs. 5 and 6. From Figs. 13 and 14 we first note that the m-dependence of $G_s(t)/G(0)$ is relatively modest in all cases. For CO_2 the m-dependence of $G_s(t)/G(0)$ parallels the behavior observed for $G(t)/G(0)$. As would be anticipated from the near equality of $G_s(t)$ and $G(t)$, in the component functions one also observes $G^{\mathrm{rot}}(t)\cong G_s^{\mathrm{rot}}(t)$ and $G^{\mathrm{trans}}(t)\cong G_s^{\mathrm{trans}}(t)$ for all m. In CH_3CN, this similarity holds in the case of the translational solvation velocity TCFs, but *not* for the rotational functions. While $G^{\mathrm{rot}}(t)$ and $G_s^{\mathrm{rot}}(t)$ are reasonably similar in the $m=3/CH_3CN$ system, the two functions become increasingly divergent as m decreases. For the $m=0$ perturbation in CH_3CN, $G^{\mathrm{rot}}(t)$ exhibits a pronounced oscillatory character, which is not present, or at least greatly muted, in its single-molecule counterpart $G_s^{\mathrm{rot}}(t)$. These os-

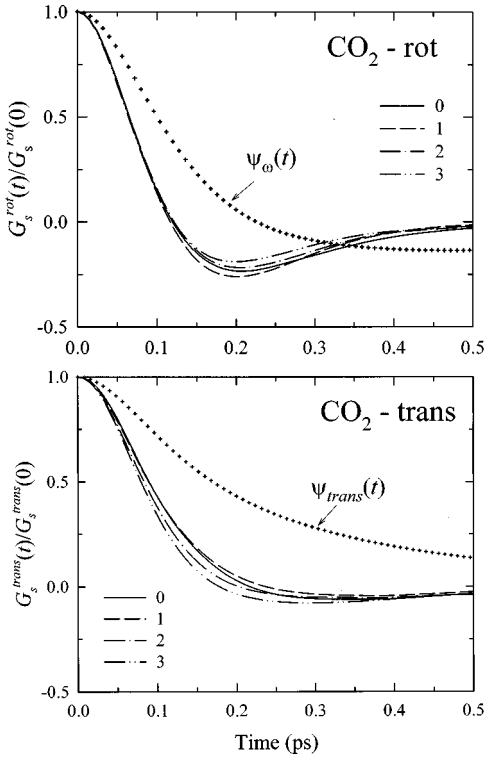

FIG. 14. Same as Fig. 13, but for the CO_2 solvent.

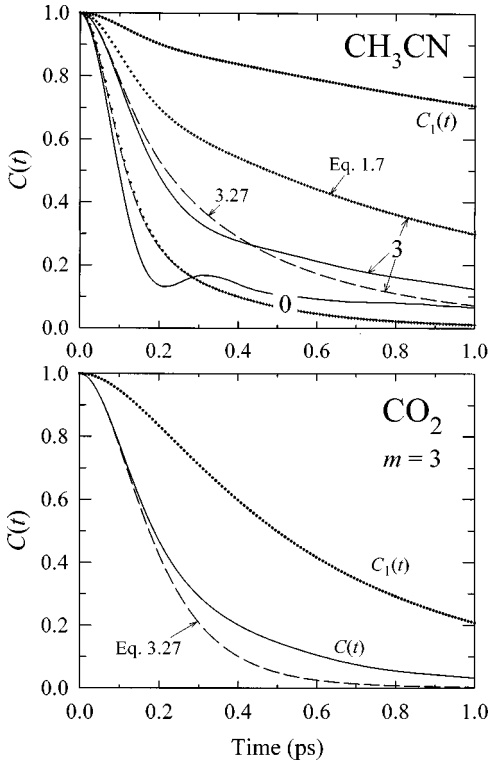

FIG. 15. Test of approximate relation, Eq. (3.27). Full lines denote the exact $C(t)$, the dashed lines its approximation via Eq. (3.27) and the crosses its approximation as $[C_1(t)]^{\alpha_1}$ (the analogue of Eq. (3.27) neglecting translational contributions). Dotted lines depict the pure-solvent orientational TCF $C_1(t)$. The CH_3CN solvation results (top panel) are for $m=0$ and $m=3$, while the CO_2 results (bottom panel) are only for $m=3$.

cillations, which ultimately produce the difference between $G_s(t)$ and $G(t)$, are undoubtedly related to contributions of coupled librational motions to $G_p(t)$. While the present type of analysis has not been carried out on many other systems, the influence of correlated librational motion is a characteristic feature of low-m solvation[30] and longitudinal relaxation[70–74] in highly dipolar liquids, which often display oscillatory TCFs. Compared to a nondipolar liquid such as CO_2, solvent molecules in highly polar liquids like CH_3CN experience much larger restoring torques, which enhance the librational character of rotational motion (see below). More importantly, the strong dipole–dipole coupling between such molecules leads to correlations between the librations on adjacent solvent molecules that are largely absent in nondipolar liquids.

Given the obvious importance of dynamical pair correlations in solvation in polar liquids like CH_3CN, it is remarkable that Eq. (3.18) works as well as it does. Neglect of $G_p(t)$ leads to the inability of Eq. (3.18) to predict the oscillations present in the $C(t)$ $m=0/CH_3CN$ system shown in Fig. 11. However, as already noted, the remaining features of $C(t)$ are in fact well accounted for. We conclude then that *dynamical* correlations of this sort play a much less critical role in determining the essential features of the solvation response than do the static aspects of intermolecular correlations captured in α_s.

In view of the reasonable accuracy shown by this first level of approximation, we now consider the further approximations embodied in Eq. (3.27). Although Eq. (3.27) is expected to be less accurate than Eq. (3.18), it provides an approximate description of solvation dynamics in terms of simple single-molecule motions present in the neat solvent. To the extent that such a description is reliable, it allows different kinds of collective dynamics (i.e., solvation dynamics, polarizability anisotropy dynamics, dielectric relaxation) to be inter-related via only the two basic dynamical functions $\psi_{\rm rot}(t)$ and $\psi_{\rm trans}(t)$ and equilibrium quantities like $\langle \delta\Delta E^2\rangle$, $G_{\rm rot}(0)$, and $G_{\rm trans}(0)$.

Figure 15 tests Eq. (3.27) against data for the $m=0$ and $m=3$ solutes in CH_3CN and the $m=3$ solute in CO_2. Also shown in this figure are tests of the equivalent of Eq. (1.7), which is what is obtained from Eq. (3.27) by neglecting translational contributions to the dynamics. First consider the CH_3CN results. Comparing Figs. 15 and 11, one finds that Eq. (3.27) captures the solvation response in CH_3CN as well, or perhaps slightly better than Eq. (3.18). While the oscillatory features of the $m=0$ response are not reproduced here either (since dynamical correlations are again ignored), the remaining characteristics of $C(t)$ are reasonably accounted for. At all values of m, both the width and amplitude of the initial Gaussian feature in $C(t)$, as well the timescale of the diffusive tail, appear to be reasonably captured by this approximation. As would be expected, neglect of the translational contribution of the response, i.e., substituting Eq. (1.7) for (3.27), yields generally poorer agreement with the observed $C(t)$ functions. The exception to this statement is the $m=0$ perturbation. As we have shown in part B, >90% of the initial solvation response is rotational, so that in this case neglect of the translational contribution leads to an almost imperceptible effect on the predicted response (Fig. 15). As

has been shown numerous times before, the simple relation $C(t) \cong \{C_1(t)\}^{\alpha_1}$ does account for the basic features of the response to an ionic perturbation. But for higher-order perturbations, where translation is no longer such a small fraction of the response, Eq. (1.7) is definitely inferior to Eq. (3.27). For the octupolar perturbation ($m=3$) displayed in Fig. 15 the translational contribution speeds up the response by about a factor of 2 compared to the rotation-only case. This observation, that translation speeds up solvation dynamics, confirms the predictions of several theoretical treatments.[63–66] However, it should be noted that these theories were formulated in terms of translational diffusion and, unlike Eq. (3.27), do not correctly predict the contributions of solvent translation to the short time dynamics.

Cursory examination of the CO_2 data in Fig. 15 might lead one to conclude Eq. (3.27) is about as good an approximation in CO_2 as it is in CH_3CN. However, a closer inspection reveals that, in contrast to the CH_3CN case, Eq. (3.27) severely underestimates the amplitude of the diffusive tail of $C(t)$. [The tail accounts for roughly 60% of the real $C(t)$ but it is only 30% in the predicted function.] This perhaps subtle distinction between the quality of the predictions of Eq. (3.27) in the cases of CO_2 and CH_3CN is the result of a more fundamental distinction between these two solvents. Whereas the further assumptions required to obtain Eq. (3.27) from Eq. (3.18) appear to be reasonable in the case of CH_3CN, in CO_2 they do not.

One key assumption used in deriving Eq. (3.27) is that all necessary dynamical information for calculation of $C(t)$ can be obtained from the pure-solvent functions $\psi_{\rm rot}(t)$ and $\psi_{\rm trans}(t)$, i.e., that $G(t)$ can be approximated by Eq. (3.23). In the case of CH_3CN this approximation appears to be no more or less valid than the approximation $G(t) \cong G_s(t)$. This fact is illustrated by the remarkable agreement between the (normalized functions) $G_s^{\rm rot}(t)$ and $\psi_\omega(t) \cong \psi_{\rm rot}(t)$ and between $G_s^{\rm trans}(t)$ and $\psi_{\rm trans}(t)$ displayed in Fig. 13. To a reasonable first approximation, all of the $G_s(t)$ functions for different m values are identical to one another and are also close to their respective pure-solvent functions $\psi(t)$. In CH_3CN one can therefore picture solvation dynamics in terms of these basic solvent-molecule motions $\psi_{\rm rot}(t)$ and $\psi_{\rm trans}(t)$ which translate into the collective solvation response, primarily via the static factors $G^{\rm rot}(0)$, $G^{\rm trans}(0)$, and $\langle \delta \Delta E^2 \rangle$. The hope that one can understand a variety of different collective TCFs in CH_3CN in this same manner is underscored by the striking similarity previously shown for the $G^{\rm rot}(t)$ and $G^{\rm trans}(t)$ functions associated with the collective polarizability and solvation response functions in CH_3CN.[24]

In contrast to this simple scenario in CH_3CN, Fig. 14 shows that the approximations $G_s^{\rm rot}(t)/G_s^{\rm rot}(0) \cong \psi_{\rm rot}(t)$ and $G_s^{\rm trans}(t)/G_s^{\rm trans}(0) \cong \psi_{\rm trans}(t)$ are unacceptable in the case of CO_2. Both of the simple velocity TCFs of the pure-solvent decay much more slowly that do the corresponding solvation velocity functions (which again are nearly m-independent). Use of these more slowly decaying functions in Eq. (3.27) is the reason that much too small a diffusive tail is predicted in $C(t)$.

It is interesting that the solvation velocity functions $G_s^{\rm rot}(t)$ and $G_s^{\rm trans}(t)$ are similar in CO_2 and CH_3CN, whereas the solvent molecule velocity functions are rather different. In CO_2 both $\psi_\omega(t)$ and $\psi_{\rm trans}(t)$ exhibit much slower initial decay than in CH_3CN. $\psi_\omega(t)$ has a considerably more shallow negative region, indicating that reversal of the direction of the molecular angular velocity ω_j due to recoil from the surrounding cage of neighbors is much less pronounced than in CH_3CN. Unlike in CH_3CN, $\psi_{\rm trans}(t)$ in CO_2 exhibits no negative region, indicating that the center-of-mass velocity vectors $\mathbf{v}_j$ do not suffer appreciable recoil. These differences in the characteristics of the velocity TCFs in the two liquids are indicative of the differences in strength of intermolecular forces that give rise to local structure and the resulting cage effects on the dynamics.[78] Although their constituent molecules are similar in nearly every other aspect, the dipolar symmetry of CH_3CN compared to the quadrupolar symmetry of CO_2 leads to CH_3CN being a much more strongly bound liquid under the same temperature and density conditions. (For example, the total binding energies in the CH_3CN simulations are 34 kJ/mol compared to 9 kJ/mol in CO_2.) The stronger interactions in CH_3CN lead to both faster decay of $\psi_\omega(t)$ and $\psi_{\rm trans}(t)$ and slower translational and reorientational motion compared to CO_2. [See for example the differences between $C_1(t)$ displayed in Fig. 15.]

These last two features of the dynamics in CO_2 as compared to CH_3CN probably underlie the breakdown of Eq. (3.27) and its precursor Eq. (3.23) in the case of CO_2. While there are several approximations made in progressing from the exact $G(t)$ [Eq. (3.21)] to its approximation in terms of $\psi_{\rm rot}(t)$ and $\psi_{\rm trans}(t)$, the most likely source the difficulty is in the evaluation of all derivatives of ΔE at their time-zero values, i.e., the assumption $D_{i\mu}(0)\, D_{i\mu}(t) \cong [D_{i\mu}(0)]^2$. This approximation is accurate when the velocity terms $\langle \dot{r}_{i\mu}(0) \dot{r}_{i\mu}(t) \rangle$ in Eq. (3.23) decay much more quickly than these positional derivative (force and torque) terms. Evidently, in CH_3CN, and judging from the widespread applicability of Eq. (1.7) in many other highly polar liquids as well, solvent molecule velocities decay fast enough compared to positions and orientations that neglect of the time dependence of these $D_{i\mu}$ terms is acceptable. In the nondipolar solvent CO_2, the slower decay of these velocity terms [i.e., $\psi_{\rm rot}(t)$ and $\psi_{\rm trans}(t)$] coupled to faster net reorientation and translation renders this timescale separation invalid.

V. SUMMARY AND CONCLUSIONS

In this paper we have presented an investigation into the molecular mechanisms of solvation dynamics for polyatomic solutes in polar and nondipolar liquids. The particular systems studied consisted of a models of a benzenelike solute in the solvents acetonitrile and carbon dioxide under the conditions of room temperature (298 K) and a volume of 52.18 cm^3/mol (the volume of acetonitrile at atmospheric pressure.) Molecular dynamics simulations were used to obtain the solvation TCFs, $C(t)$, for a set of perturbations ΔE in the solute-solvent electrostatic potential, corresponding to multipolar ($m=0-3$) changes in the solute charge distribution (Fig. 1). This choice of solute and this form of perturbation were motivated by the fact that the chromophores

typically used in solvation dynamics experiments are large polyatomic molecules in which the $S_0 \rightarrow S_1$ electronic transition involves charge redistribution among many solute atoms. Our study of solvation mechanisms focused on answering two questions: First, how is the solvent response divided between rotational and translational dynamics? Second, how collective is solvation dynamics? By finding out how the answers depend on the form of ΔE and on the solvent we were also able to determine why $C(t)$ varies with the change in the solute charge distribution and with solvent polarity.

Information about the relative importance of rotational and translational solvent motions in the solvation response was derived from the solvation velocity TCF, $G(t) = \langle \Delta \dot{E}(0) \Delta \dot{E}(t) \rangle$, and its decomposition into rotational and translational components. Examination of the single-molecule contributions to $G(t)$ served as a starting point for deriving several approximations to $C(t)$ in terms of single-molecule dynamics through application of the general formalism developed by Steele.[49] The MD data were then used to examine the validity of these approximations.

With respect to solvation mechanisms our main findings are:

(1) Solvation dynamics is much more collective in polar (CH_3CN) than in nondipolar (CO_2) fluids. This is illustrated most dramatically by the results presented in Figs. 9 and 10, especially for an ionic ($m=0$) perturbation in the solute-solvent interactions. The very rapid decay of $C(t)$ in acetonitrile is due to the almost complete cancellation of the single-molecule contribution $[C_s(t)]$ to the solvation TCF by the pair contribution $[C_p(t)]$. In CO_2, on the other hand, such cancellation has a minor effect on $C(t)$. This much more important role of solvent-solvent correlations in the dipolar case appears to be the main source of differences in electrostatic solvation dynamics in polar and nondipolar liquids.

(2) The collective nature of solvation dynamics is due mainly, but not entirely, to static solvent–solvent correlations. This can be seen by contrasting the very large contribution of $C_p(t)$ to $C(t)$ in acetonitrile with the relatively more modest contribution of $G_p(t)$ to its solvation velocity TCF $G(t)$.

(3) Contributions to solvation dynamics from collective dynamical correlations are primarily rotational and significant only in polar solvents. This is illustrated in the comparisons of the $G(t)$ (Figs. 5 and 6) with $G_s(t)$ (Figs. 13 and 14) in the two liquids. The fact that dynamical correlations in a polar solvent are primarily rotational is consistent with the fact that such correlations arise mainly through dipole–dipole interactions.

(4) Solvation dynamics is less collective at larger m. This conclusion is based primarily on the acetonitrile results, given that for CO_2 the solvation response is dominated by $C_s(t)$ at all m. In CH_3CN the decreasing collectivity manifests itself through the decrease of α_s (Table II) and of the extent of cancellation of $C_s(t)$ by $C_p(t)$ with increasing m. This trend is consistent with the diminishing importance of solvent–solvent correlations as the range of ΔE decreases.

(5) The contribution of translational solvent motions to the solvation response increases with increasing m (Figs. 3 and 4). This trend is independent of solvent polarity and is also related to the decrease in the effective range of ΔE with increasing m. For short time solvation dynamics, characterized by the solvation frequency ω_s, the translational contribution to ω_s^2 ranges from around 8% to 41% as m increases from 0 to 3 (Table II and Figs. 7 and 8). This finding has important implications for theories of solvation dynamics using experimentally accessible pure-solvent dynamics as input. For example, in highly polar liquids, the frequency-dependent dielectric permittivity, $\epsilon(\omega)$, is dominated by rotational relaxation[71,74] and would thus not accurately describe the solvent response to quadrupolar and octopolar perturbations in the solute charge distribution. Solvent translation is also likely to make a significant contribution to solvation dynamics for large chromophores such as C153 for which ΔE corresponds to a change in many partial charges separated by distances larger than typical solvent dimensions.[23] We note that while the increase in the translational contribution enhanced the rate of decay of $C_s(t)$ with increasing m, in polar liquids $C(t)$ still decays more slowly at higher m because the less complete cancellation between $C_s(t)$ and $C_p(t)$ is the dominant effect of the increase in the multipolar order of ΔE. In CO_2, the two effects are of nearly equal importance, leading to the lack of significant m-dependence in $C(t)$. With respect to these findings, it is worth remarking that translational solvent modes motions were also found to be the primary relaxation mechanism in the case of electron solvation. Here, the influence of the changes in cavity shape greatly heightens the importance of translational solvent motions even for low-m processes.[79]

We have examined several approximate relationships between the collective dynamics of solvation and simpler, single-solvent-molecule dynamics. The first relationship, $C(t) \cong \{C_s(t)/C_s(0)\}^{\alpha_s}$, results from neglect of dynamical correlations between solvent molecules $[G_p(t)]$ and application of the cumulant approximation. Apart from the librational oscillations evident in $C(t)$ in the $m=0/CH_3CN$ case, this approximation captures the essential features of the complete solvation response in all ΔE/solvent combinations studied here. The soundness of this approximation underscores the conclusion that while solvation dynamics is a highly cooperative process in polar fluids, the collective aspects reside primarily in static (α_s) rather than dynamical $[G_p(t)]$ intermolecular correlations.

A more approximate expression for $C(t)$ can be derived by equating the dynamics contained in $G_s(t)$ to the dynamics of simple rotation and translation of solvent molecules in the absence of the solute [Eq. (3.27)]. Among other things, this second level of approximation requires that solvent molecule velocities become uncorrelated much more quickly than the electrostatic forces and torques between the solute and a solvent molecule. In the highly polar liquids like CH_3CN this condition appears to be met. It is therefore possible to semiquantitatively describe the solvation response in terms of static correlations and the dynamical information contained in the center-of-mass velocity and angular velocity autocorrelation functions of solvent molecules in the neat fluid. In the case of the $m=0$ perturbation, where rotational dynamics dominate, one can neglect translational motion alto-

gether in which case Eq. (3.27) reduces to the power-law relation between $C(t)$ and the dipole autocorrelation function $C_1(t)$, Eq. (1.7), already shown to be valid for ionic perturbations in a number of polar solvents.[35,47,51,77] For multipolar perturbations of higher order translational contributions cannot be neglected and the full expression, Eq. (3.27), should be used.

In CO_2, the conditions required for application of Eq. (3.27) are not met. In this solvent, the absence of strong dipole–dipole forces leads to slower velocity relaxation and faster net solvent displacement such that the timescale separation required in this approximation is violated. We conjecture that this failure of Eq. (3.27) in the case of CO_2 may be representative of the behavior of low-polarity solvents and polar solvents under conditions of low density, such as occur in supercritical fluids.[80] In such systems the simple and intuitively pleasing description afforded by Eq. (3.27) may not be useful.

However, at least in highly polar solvents, it appears that the approach we have demonstrated here for connecting solvation to pure-solvent dynamics is well suited to systematically studying how different dynamical processes in a given medium are inter-related. The present approach extends the connections established through the INM influence spectra characterizing these processes[7,24,25,44,46,48] to much longer times. It thus provides the means of developing, via molecular theory or simulation, the criteria under which solvation dynamics or vibrational relaxation in a given fluid can be predicted from its dielectric permittivity or its optical Kerr effect response.

ACKNOWLEDGMENT

Mark Maroncelli wishes to thank the Office of Basic Energy Sciences of the U.S. Department of Energy and Branka Ladanyi the National Science Foundation (Grant No. CHE-9520619) for support of this research.

[1] References 2–7 contain reviews of recent research advances in solvation dynamics.
[2] J. D. Simon, Acc. Chem. Res. **21**, 128 (1988).
[3] S. Ravichandran and B. Bagchi, Int. Rev. Phys. Chem. **14**, 271 (1995); B. Bagchi and A. Chandra, Adv. Chem. Phys. **80**, 1 (1991); B. Bagchi, Annu. Rev. Phys. Chem. **40**, 115 (1989).
[4] W. Jarzeba, G. C. Walker, A. E. Johnson, and P. F. Barbara, Chem. Phys. **152**, 57 (1991); P. F. Barbara and W. Jarzeba, Adv. Photochem. **15**, 1 (1990).
[5] M. Maroncelli, J. Mol. Liq. **57**, 1 (1993); M. Maroncelli, P. V. Kumar, A. Papazyan, M. L. Horng, S. J. Rosenthal, and G. R. Fleming, in *Ultrafast Reaction Dynamics and Solvent Effects*, edited by P. J. Rossky and Y. Gauduel (AIP Conference Proceedings 298, AIP, New York, 1994).
[6] G. R. Fleming and M. Cho, Annu. Rev. Phys. Chem. **47**, 109 (1996).
[7] R. M. Stratt and M. Maroncelli, J. Phys. Chem. **100**, 12981 (1996).
[8] References 9–12 contain reviews of recent research progress in dynamic solvent effects on charge-transfer processes.
[9] H. Heitele, Angew. Chem. Int. Ed. Engl. **32**, 359 (1993).
[10] J. T. Hynes, in *Ultrafast Dynamics of Chemical Systems*, edited by J. D. Simon (Kluwer, Dordrecht, 1994), pp. 345–381; B. B. Smith, H. J. Kim, D. Borgis, and J. T. Hynes, in *Dynamics and Mechanism of Photoinduced Electron Transfer*, edited by N. Mataga, T. Okada, and H. Masuhara (Elsevier, Amsterdam, 1992), pp.39–56.
[11] P. J. Rossky and J. D. Simon, Nature (London) **370**, 263 (1994).
[12] P. F. Barbara, T. J. Meyer, and M. Ratner, J. Phys. Chem. **100**, 13148 (1996).
[13] M. Maroncelli and G. R. Fleming, J. Chem. Phys. **89**, 5044 (1988).
[14] J. S. Bader and D. Chandler, Chem. Phys. Lett. **157**, 501 (1989).
[15] R. M. Levy, D. B. Kitchen, J. T. Blair, and K. Krogh-Jespersen, J. Phys. Chem. **94**, 4470 (1990); M. Belhadj, D. B. Kitchen, J. T. Blair, K. Krogh-Jespersen, and R. M. Levy, *ibid.* **95**, 1082 (1991).
[16] K. Ando and S. Kato, J. Chem. Phys. **95**, 5966 (1991).
[17] P. V. Kumar and B. L. Tembe, J. Chem. Phys. **97**, 4356 (1992).
[18] P. Muiño and P. R. Callis, J. Chem. Phys. **100**, 4093 (1994).
[19] D. B. Bursulaya, D. A. Zichi, and H. J. Kim, J. Phys. Chem. **99**, 10069 (1995); *ibid.* **100**, 1392 (1996).
[20] M. S. Skaf and B. M. Ladanyi, J. Phys. Chem. **100**, 18258 (1996).
[21] M. Maroncelli, J. Chem. Phys. **94**, 2084 (1991).
[22] B. M. Ladanyi and R. M. Stratt, J. Phys. Chem. **99**, 2502 (1995).
[23] P. V. Kumar and M. Maroncelli, J. Chem. Phys. **103**, 3038 (1995).
[24] B. M. Ladanyi and S. Klein, J. Chem. Phys. **105**, 1552 (1996).
[25] B. M. Ladanyi and R. M. Stratt, J. Phys. Chem. **100**, 1226 (1996).
[26] B. M. Ladanyi, in *Electron Transfer in Condensed Media*, edited by A. A. Kornyshev and J. Ulstrup (World Scientific, Singapore, 1997), pp. 110–129.
[27] E. A. Carter and J. T. Hynes, J. Chem. Phys. **94**, 5961 (1991).
[28] S. J. Rosenthal, X. Xie, M. Du, and G. R. Fleming, J. Chem. Phys. **95**, 4715 (1991).
[29] S. J. Rosenthal, R. Jimenez, G. R. Fleming, P. V. Kumar, and M. Maroncelli, J. Mol. Liq. **60**, 25 (1994).
[30] R. Jimenez, G. R. Fleming, P. V. Kumar, and M. Maroncelli, Nature (London) **369**, 471 (1994).
[31] J. Gardecki, M. L. Horng, A. Papazyan, and M. Maroncelli, J. Mol. Liq. **65/66**, 49 (1995).
[32] M. L. Horng, J. Gardecki, A. Papazyan, and M. Maroncelli, J. Phys. Chem. **99**, 17311 (1995).
[33] D. Bingemann and N. Ernsting, J. Chem. Phys. **102**, 2691 (1995).
[34] Most MD simulation studies of solvation dynamics have addressed some aspects of the solvation mechanism. For an overview of many of the more important results, see Ref. 7.
[35] R. Brown, J. Chem. Phys. **102**, 9059 (1995).
[36] K. Ando, J. Chem. Phys. **107**, 4585 (1997).
[37] F. O. Raineri, H. L. Friedman, and B.-C. Perng, J. Mol. Liq. **73**, 419 (1997).
[38] X. Song and D. Chandler, J. Chem. Phys. **108**, 2594 (1998).
[39] S.-G. Su and J. D. Simon, J. Phys. Chem. **93**, 753 (1989).
[40] C. F. Chapman, R. S. Fee, and M. Maroncelli, J. Phys. Chem. **99**, 4811 (1995).
[41] Exceptions are Refs. 25, 26, and: B.-C. Perng, M. D. Newton, F. O. Raineri, and H. L. Friedman, J. Chem. Phys. **104**, 7153,7177 (1996); D. V. Matyushov, R. Schmid, and B. M. Ladanyi, J. Phys. Chem. B **101**, 1035 (1997).
[42] L. Reynolds, J. A. Gardecki, S. J. V. Frankland, M. L. Horng, and M. Maroncelli, J. Phys. Chem. **100**, 10337 (1996).
[43] R. M. Stratt and M. Cho, J. Chem. Phys. **100**, 6700 (1994).
[44] R. M. Stratt, Acc. Chem. Res. **28**, 201 (1995).
[45] T. S. Kalbfleisch, L. D. Ziegler, and T. Keyes, J. Chem. Phys. **105**, 7034 (1996).
[46] R. E. Larsen, E. F. David, G. Goodyear, and R. M. Stratt, J. Chem. Phys. **107**, 524 (1997).
[47] M. Re and D. Laria, J. Phys. Chem. B **101**, 10494 (1997).
[48] B. M. Ladanyi and R. M. Stratt, J. Phys. Chem. A **102**, 1068 (1998).
[49] W. A. Steele, Mol. Phys. **61**, 1031 (1987).
[50] H. Stassen and W. A. Steele, J. Phys. Chem. B **101**, 8774 (1997).
[51] M. Maroncelli, P. V. Kumar, and A. Papazyan, J. Phys. Chem. **97**, 13 (1993). See also the discussion in A. Papazyan and M. Maroncelli, J. Chem. Phys. **95**, 9219 (1991), Sec. IV B.
[52] E. W. Castner, Jr. and M. Maroncelli, J. Mol. Liq. **77**, 1 (1998).
[53] F. O. Raineri and H. L. Friedman, J. Chem. Phys. **101**, 6111 (1994).
[54] M. P. Allen and D. J. Tildesley, *Computer Simulation of Liquids* (Oxford, New York, 1989).
[55] D. M. F. Edwards, P. A. Madden, and I. R. McDonald, Mol. Phys. **51**, 1141 (1984).
[56] J. G. Harris and K. H. Yung, J. Phys. Chem. **99**, 12021 (1995). The authors do not use the arithmetic mean to determine σ_{CO}, but use $\sigma_{CO}=(\sigma_O\sigma_C)^{1/2}$ instead. However the two set of values differ only by about 0.1%. Equation (2.1) gives $\sigma_{CO}=2.895$ Å, while $(\sigma_O\sigma_C)^{1/2}=2.892$ Å.
[57] D. J. Adams and G. S. Dubey, J. Comput. Phys. **72**, 156 (1987).
[58] A. J. C. Ladd, Mol. Phys. **36**, 463 (1978); M. Neumann, O. Steinhauser, and G. S. Pawley, *ibid.* **52**, 97 (1984).

[59] M. Buchner, B. M. Ladanyi, and R. M. Stratt, J. Chem. Phys. **97**, 8522 (1992).
[60] Cumulant approximations to time correlations are discussed in a number of articles and books. See, for example, W. G. Rothschild, *Dynamics of Molecular Liquids* (Wiley, New York, 1984), Chap. 3 and Appendix H.
[61] See Fig. 5 of Ref. 59 for a comparison of $\psi_{\mathrm{rpt}}(t)$ and $\psi_{\omega}(t)$. It is shown there that the two are nearly identical when θ_j and $\dot{\phi}_j$ relax rapidly relative to angular displacements.
[62] Cumulant approximations to orientational TCFs are described by R. M. Lynden-Bell, in *Molecular Liquids: Dynamics and Interactions*, edited by A. J. Barnes, W. J. Orville-Thomas, and J. Yarwood (D. Reidel, Dordrecht, 1984), pp. 501–508; and R. M. Lynden-Bell and W. A. Steele, J. Phys. Chem. **88**, 6514 (1984).
[63] G. van der Zwan and J. T. Hynes, J. Phys. Chem. **89**, 4181 (1985).
[64] B. Bagchi and A. Chandra, J. Chem. Phys. **90**, 7338 (1989); A. Chandra and B. Bagchi, Proc.-Indian Acad. Sci., Chem. Sci. **101**, 83 (1989); A. Chandra and B. Bagchi, J. Phys. Chem. **93**, 6996 (1989).
[65] L. E. Fried and S. Mukamel, J. Chem. Phys. **93**, 932 (1990).
[66] D. Wei and G. N. Patey, J. Chem. Phys. **93**, 1399 (1990).
[67] J. G. Saven and J. L. Skinner, J. Chem. Phys. **99**, 4391 (1993).
[68] G. Birnbaum and B. Guillot, in *Collision- and Interaction-Induced Spectroscopy*, edited by G. C. Tabisz and M. N. Neuman (Kluwer, Dordrecht, 1995).
[69] F. O. Raineri, Y. Zhou, H. L. Friedman, and G. Stell, Chem. Phys. **152**, 189 (1991).
[70] D. Bertolini and A. Tani, Mol. Phys. **75**, 1065 (1992).
[71] M. S. Skaf, T. Fonseca, and B. Ladanyi, J. Chem. Phys. **98**, 8929 (1993).
[72] B. M. Ladanyi and M. S. Skaf, J. Phys. Chem. **100**, 1368 (1996).
[73] D. M. F. Edwards and P. A. Madden, Mol. Phys. **51**, 1163 (1984).
[74] R. W. Impey, P. A. Madden, and I. R. McDonald, Mol. Phys. **46**, 513 (1982).
[75] The cancellation is demonstrated in the static case of the charge-charge structure factor by F. O. Raineri, H. Resat, and H. L. Friedman, J. Chem. Phys. **96**, 3068 (1992); P. A. Bopp, A. A. Kornyshev, and G. Sutmann, Phys. Rev. Lett. **76**, 1280 (1996); M. S. Skaf, Mol. Phys. **90**, 25 (1997).
[76] For the longitudinal dipole density TCF, the physical reasons for the cancellation are discussed by D. Kivelson and H. L. Friedman, J. Phys. Chem. **93**, 7026 (1989). The cancellation of the self- and distinct components of this TCF is demonstrated for supercooled water in Ref. 70. Similar cancellation occurs for the corresponding components of the charge density TCF of room-temperature acetonitrile (B.-C. Perng and B. M. Ladanyi, to be submitted).
[77] R. Olender and A. Nitzan, J. Chem. Phys. **102**, 7180 (1995).
[78] The articles cited in Ref. 62 contain discussions of the intermolecular potential and thermodynamic state dependence of the angular velocity TCF. For a corresponding discussion of the behavior of the center-of-mass velocity TCF, see, for example, J. P. Hansen and I. R. McDonald, *Theory of Simple Liquids*, 2nd ed. (Academic, Orlando, FL, 1986), Chap. 7.
[79] See for example, B. J. Schwartz and P. J. Rossky, J. Chem. Phys. **101**, 6902 (1994); P. Graf, A. Nitzan, and G. H. F. Diercksen, J. Phys. Chem. **100**, 18916 (1996).
[80] Note, however, that this may not be the case in supercritical water, where Re and Laria (Ref. 47) recently observed that the relation $C(t) \cong \{C_1(t)\}^{\alpha_1}$ holds even at very low densities.